St. John's University

St. John's Scholar

Theses and Dissertations

2022

TEPOTINIB REVERSES ABCB1- AND ABCG2-MEDIATED MULTIDRUG RESISTANCE IN CANCER

Zhuoxun Wu

TEPOTINIB REVERSES ABCB1- AND ABCG2-MEDIATED MULTIDRUG

RESISTANCE IN CANCER

A dissertation submitted in partial fulfillment

of the requirements for the degree of

DOCTOR OF PHILOSOPHY

to the faculty of the

DEPARTMENT OF PHARMACEUTICAL SCIENCES

of

COLLEGE OF PHARMACY AND HEALTH SCIENCES

at

ST. JOHN'S UNIVERSITY

New York

by

Zhuoxun Wu

Date Submitted: ___04/19/2022___   Date Approved: ___03/13/2023___

_____   _____

Zhuoxun Wu   Dr. Zhe-Sheng Chen

ABSTRACT

TEPOTINIB REVERSES ABCB1- AND ABCG2-MEDIATED MULTIDRUG RESISTANCE IN CANCER

Zhuoxun Wu

Overexpression of ATP-binding cassette (ABC) transporters ABCB1 and ABCG2 in cancer cells have been linked to the development of multidrug resistance (MDR), an obstacle to cancer therapy. Therefore, it is important to inhibit ABCB1/ABCG2 activity in order to maintain an effective intracellular level of chemotherapeutic drugs in drug-resistant cancer cells. Tepotinib is an ATP-competitive MET kinase inhibitor approved for the treatment of adult patients with metastatic non–small cell lung cancer harboring *MET* exon 14 skipping alterations. In the present study, we identified that the MET inhibitor tepotinib can reverse ABCB1- and ABCG2-mediated MDR by directly binding to the drug-binding site of the transporters and reversibly inhibiting drug efflux activity, therefore enhancing the cytotoxicity of substrate drugs in drug-resistant cancer cells. Furthermore, the *ABCB1/ABCG2* double-transfected cell model and *ABCG2* gene knockout cell model demonstrated that tepotinib specifically inhibits these two MDR-related ABC transporters. The ATPase assay showed that tepotinib concentration-dependently inhibited the ATPase activity of ABCB1 but stimulated the ATPase activity of ABCG2. Furthermore, treatment with tepotinib did not alter protein expression or subcellular localization of ABCB1/ABCG2. The docking simulation suggested a high binding affinity of tepotinib with ABCB1/ABCG2 drug-binding site. In mouse bearing drug-resistant tumors, tepotinib increased the intratumoral accumulation of ABCG2 substrate drug topotecan and enhanced its antitumor effect. Taken together, our study

provides a new potential of repositioning tepotinib as a dual ABCB1/ABCG2 inhibitor and combining tepotinib with substrate drugs to antagonize MDR.

ACKNOWLEDGEMENT

My Ph.D. program in St. John's wouldn't have been so smooth and pleasurable without help from many individuals. It is a pleasure to convey my gratitude to them in my humble acknowledgement.

Firstly, I would like to express my deepest thank to my mentor, Dr. Zhe-Sheng Chen, for his supervision, advice, and guidance. He has helped me to grow as a person, student, and future scientist. Without his insightful minds, patient guidance, and dedicated involvement in every step throughout the research, I would have never been able to make such progress. I am thankful to my committee members Dr. John N.D. Wurpel, Dr. Sandra E. Reznik, Dr. Sabesan Yoganathan, and Dr. Ketankumar Patel for reviewing my thesis as well as serving as members of my Ph.D. thesis defense. I appreciate all the valuable advice in science discussions and critical comments for the project.

I am grateful to the Department of Pharmaceutical Sciences, College of Pharmacy and Health Sciences, St. John's University for allowing me to commence this thesis, to use departmental equipment, and providing graduate fellowship. I am thankful to all colleagues and laboratory members for their help and support during my research and maintained a wonderful lab environment.

Finally, a very special gratitude goes to my wife Xuanyu Chen, my parents, Mr. Yuping Wu, and Mrs. Weibing Liu. This journey would not have been accomplished smoothly without their unconditional love, understanding and encouragement.

TABLE OF CONTENTS

LIST OF TABLES

LIST OF FIGURES

LIST OF ABBREVIATIONS

ABC transporter: ATP-binding cassette transporter

ABCB1: ATP-binding cassette sub-family B member 1

ABCG2: ATP-binding cassette super-family G member 2

ATP: Adenosine triphosphate

DMEM: Dulbecco's modified Eagle medium

DAPI: 4′,6-diamidino-2-phenylindole

DMSO: Dimethyl sulfoxide

EMEM: Eagle's minimum essential medium

FBS: Fetal bovine serum

GAPDH: Glyceraldehyde 3-phosphate dehydrogenase

MDR: Multidrug resistance

MET: Mesenchymal-epithelial transition

MTT: 3-(4,5-Dimethylthiazol-2-yl)-2,5-diphenyltetrazolium bromide

NBDs: Nucleotide-binding domains

PBS: phosphate buffer saline

PVDF: Polyvinylidene fluoride

SDS: Sodium dodecyl sulfate

SDS-PAGE: Sodium dodecyl sulfate-polyacrylamide gel electrophoresis

TMDs: Transmembrane domains

TPT: Topotecan

WBCs: White blood cells

CHAPTER 1

INTRODUCTION

Cancer, characterized by uncontrolled cell growth, continues to be a leading cause of death globally. According to the American Cancer Society cancer statistics, in 2022, there will be an estimated 1.9 million new cancer cases and 0.6 million cancer-related deaths in the USA (1). The most common new cases are prostate, lung, colorectal, and breast cancer, while the most common causes of cancer death are lung, prostate, breast, and colorectal cancer. Currently, chemotherapy and targeted therapy are two mainstream cancer treatment strategies. However, the development of drug resistance, which results in decreased or diminished therapeutic response, is one of the major challenges for cancer treatment. MDR is characterized as the acquired drug resistance of cancer cells to multiple anticancer drugs even though they have distinct chemical structures or mechanisms of action (2). Although it is not completely elucidated, several mechanisms can lead to cancer MDR, including alteration of drug metabolism, inhibition of apoptosis, upregulation of efflux transporters, and increased DNA repair of cancer cells (3). It is recognized that some ATP-binding cassette (ABC) transporters can render cancer cells multidrug resistance (MDR) phenotype and attenuate the efficacy of anticancer drugs (4).

The ABC transporter superfamily contains multiple groups of active transporter proteins locate on cell membrane with crucial pharmacological and physiological functions (5). The superfamily is classified into 7 subfamilies from ABCA to ABCG (6, 7). Up to now, 49 human ABC transporters have been reported in which most of them have pharmacological and/or physiological functions (8). ABC transporters are membrane-bound efflux pumps that translocate their substrates against the concentration gradients by hydrolyzing ATP, thereby decreasing the intracellular

retention of substrate molecules (9). The well-established, MDR-associated ABC transporters are ABCB1 (P-glycoprotein, P-gp), ABCG2 (breast cancer resistance protein, BCRP), and ABCC1 (multidrug resistance-associated protein 1, MRP1) (10, 11). To dates, numerous clinically used chemotherapeutic drugs and tyrosine kinase inhibitors (TKIs) are recognized as substrate drugs of ABC transporters (12-16).

ABCB1 is the first discovered efflux transporter and is by far the most studied ABC transporter in MDR (17). The protein structure of ABCB1 was revealed by cryo-EM (18), which is a homodimer transmembrane glycoprotein with two monomers each including a transmembrane domain (TMD) with six transmembrane α-helices and a nucleotide-binding domain (NBD) where ATP is bound and hydrolyzed. Three conformations have been identified for ABCB1 including an inward facing conformation, an outward opening conformation and an occluded conformation. Interestingly, the occluded conformation prevents some substrates from access the transporter and may occur during inhibitor binding or a productive transport cycle. ABCB1 is widely distributed in the blood-brain barrier, placenta, kidneys, and intestines, where it protects the organs by pumping out the toxins from the cells (19, 20). As one of the major contributors to MDR, ABCB1 expression can be upregulated in cancer cells by long-term exposure to anticancer drugs, which inevitably causing MDR (21-23). To dates, a wide range of anticancer drugs were identified as substrates of ABCB1, including chemotherapeutic agents doxorubicin, paclitaxel, and vincristine (24), as well as tyrosine kinase inhibitors palbociclib (25), and imatinib (26).

ABCG2 was discovered by several groups successively. Doyle LA and colleague reported overexpression of ABCG2 in MCF-7/AdVp3000 and they termed it as breast cancer resistance protein (BCRP) (27). Later, the ABCG2 cDNA was cloned from S1-M1-80 cancer cell line and termed MXR (28). Based on the structure and arrangement

of NBDs and TMDs, ABCG2 is grouped into half transporter that has one NBD located in cytoplasm and one hydrophobic TMD. ABCG2 is widely distributed in normal tissues including placenta, prostate, liver, and maintained the cellular homeostasis (29). As an MDR-related ABC transporter, consistent data have suggested that ABCG2 expression predicts poor clinical outcomes in acute myelogenous leukemia, acute lymphoblastic leukemia, lung, and breast cancer (30). In accordance, Maria Et al. reported that ABCG2 is associated with the formation of side population in lung cancer cells (31). Hence, both pre-clinical and clinical data highlighted the role of ABCG2 in the development of drug resistance. Some clinical used ABCG2 substrate drugs include chemotherapeutic agents such as irinotecan, topotecan, mitoxantrone (32), and TKIs such as tivantinib (13) and pevonedistat (33). Moreover, clinical studies suggested that ABCG2 is one of the key resistance factors of sorafenib, sunitinib and erlotinib, which affect to drug pharmacokinetics and pharmacodynamics (34, 35).

ABCC1 is also known to mediate MDR in cancer cells but to a lesser extent compared to ABCB1 and ABCG2. ABCC1 was firstly isolated from doxorubicin-resistance small cell lung cancer line H69AR and its correlation with MDR was established in 1992 (36). The structural studies of ABCC subfamily are relative scarce. The cryo-EM structure of ABCC1 was reported recently, showing that it has three TMDs and two NBDs (37). ABCC1 has an additional N-terminal TMD (TMD_0) that is smaller than the core TMD (38) but the extra TMD_0 of ABCC1 is not required for the transport function (39). ABCC1 has a wide distribution in physiological tissues such as adrenal gland, bladder, choroid plexus, as well as helper T cells and muscle cells (40). It has an overlapping substrate profile as ABCB1, but it is also able to pump out organic anions such as methotrexate and arsenate (41, 42).

It has been suggested that co-expression of multiple transporters in cancer cells

may render a more pronounced MDR phenotype compared to those with single transporter overexpression, particularly in acute myeloid leukemia (AML). Wilson et al analyzed the gene expression profiles of 170 pretreated AML samples and identified that the most significant drug resistance was associated with increased co-expression of ABCB1 and ABCG2 (43). Liu et al. used bone marrow mononuclear cells from 96 de novo AML patients to test the expression of several ABC transporters, including ABCB1, ABCB4, ABCG2, ABCC1, and ABCC4 (44). The results reinforced that co-expression of multiple transporters was associated with worse prognosis. Another study compared the drug resistance-related genes from 11 pairs of patient samples obtained at diagnosis or at relapse, increased expression of ABCB1 and ABCG2 was identified in two AML relapsed patients (45). Studies also suggest that, in childhood AML patients, the possibility of remission or improvement of PFS were significantly correlated with the number of overexpressed ABC transporters (46). Therefore, dual inhibition of both ABCB1 and ABCG2 may be necessary to completely antagonize MDR in certain circumstances.

Because ABC transporters are believed to mediate MDR in cancer, the research on combating MDR by targeting these ABC transporters are ongoing. These approaches include designating drugs with novel mechanism of action or structure to bypass MDR, and the development of reversal inhibitor to block the efflux activity of ABC transporter and restore drug accumulation in MDR cancer cells. For ABCB1, three generations of inhibitor have been developed to reverse drug resistance. However, these inhibitors failed to show desired therapeutic effect in clinical settings. The first-generation inhibitor verapamil and cyclosporine A had a relatively low affinity and selectivity to ABCB1, leading to dosing and side effect problems. The second-generation inhibitors are derived from structural optimization of first-generation inhibitor, such as

dexverapamil and valspodar. These inhibitors have better affinity and selectivity compared to the first-generation inhibitors but exhibit cytochrome P450 enzyme inhibition. Thus, it is likely that they will cause drug-drug interactions when co-administrated with substrate drugs. The third-generation inhibitors tariquidar and zosuquidar were developed to further improve the potency and reduce toxicity. Unfortunately, these inhibitors did not achieve significant therapeutic effect in clinical trials despite the robust preclinical data.

Unlike the extensive clinical development of ABCB1 inhibitors, no ABCG2 inhibitor has been subjected to clinical trials to date. Fumitremorgin C is the first reported ABCG2 inhibitor with severe neurotoxicity. Later, the Fumitremorgin C analogue Ko143 was developed with stronger ABCG2 inhibitory effect and lower toxicity. However, *in vivo* rat studies showed that Ko143 can be rapid metabolized into inactive metabolite, limiting its clinical application. It is reported that some ABCB1 inhibitors such as valspodar and tariquidar also demonstrate ABCG2 inhibitory effect, while the effect has not been tested in clinical trial.

Recently, some tyrosine kinase inhibitors (TKIs) are reported to exhibit inhibitory effect to the activity of ABC transporters and thus hold promise to overcome MDR (47-51). These TKIs, such as gefitinib, nilotinib, imatinib, regorafenib, are either clinically approved or under clinical trials (49, 52). They may potentially be used as reversal agents combined with chemotherapeutic drugs to combat MDR in cancer. Particularly, one advantage of repurposing TKIs as reversal inhibitors is that the TKIs have more clinical data to predict the fate of the drugs compared to the synthetic compounds. It has been shown that these TKIs may reverse MDR via several mechanisms including 1) direct binds to the substrate-binding site of the transporter and interferes the capture of substrate drugs, 2) inhibits the ATPase function of the transporter, thus limiting the

drug efflux activity, 3) downregulates the protein expression of ABC transporter, and 4) inactivates the transporter by translocating it from cell membrane to cytoplasm.

Tepotinib is an ATP-competitive, highly selective TKI targeting to the MET receptor that under rapid development in recent years (53). The MET tyrosine kinase receptor is overexpressed or mutated in many cancer cells, regulating cellular process such as proliferation, invasion, and mobilization (54). The *MET* gene is located in human chromosome 7, encoding the MET protein. Normal expression of MET is known to maintain the tissue homeostasis, but abnormal regulation can lead to proliferation and metastasis of tumor cells. In 2005, Ma et al provided the first direct evidence that downregulating receptor expression or abrogating MET activity can inhibit cell growth in MET-expressing NSCLC cells (55). The study suggested that MET plays a crucial role in NSCLC biology and biochemistry, purposing it as a potential target for NSCLC treatment (56). In NSCLC, dysregulation of the MET pathway occurs through a variety of mechanisms, including *MET* gene mutation, gene amplification, and protein overexpression (57, 58). The METex14 skipping mutations accounts for 2-3% of NSCLCs and approximately 3% of the adenocarcinoma cases (59). It was revealed that the MET exon 14 contains Y1003, a binding site for E3-ubiquitin ligase CBL. Therefore, when exon 14 skipping occurs, the ubiquitin ligase lost the binding sites. This in turn leads to the protection of MET receptor from ubiquitination and protein degradation, resulting in sustained activation of the MET (60, 61). The MET-TKIs can be divided into three types: 1) type I inhibitors, including tepotinib and crizotinib, are ATP competitive inhibitors that bind to the active form of MET, 2) type II inhibitors such as merestinib and glesatinib are ATP competitors that bind to the inactive form of MET, 3) type III inhibitor tivantinib is an allosteric inhibitor that does not compete with ATP (62). As a type I inhibitor, tepotinib binds to MET in a U-shape geometry through

interactions with both hinge and activation loop residue Y1230, which interferes the ATP binding process. Therefore, tepotinib is able to block the constitutive phosphorylation of MET, thereby inhibiting the cell growth, survival, migration and invasion of HGF/MET-driven tumor cells (63). In addition, this mechanism of action allows tepotinib to be more selective to MET compared to type II inhibitors that can target multiple kinases (64).

Tepotinib was first reported by Bladt et al. in 2013 (63). The MET inhibition and antitumor effect were evaluated both *in vitro* and *in vivo*. Tepotinib inhibited the MET kinase activity with an average IC_{50} of 3 nM, with no significant inhibitory effect towards a panel of 242 human kinases. *In vitro*, tepotinib showed significant antiproliferative effect to MET-addicted cancer cell lines, while higher concentrations were needed for cancer cell lines with low MET level. *In vivo*, tepotinib inhibited MET phosphorylation and demonstrated anticancer efficacy in MET-driven tumor xenograft models. Preclinical data also revealed that tepotinib has radiosensitize effect when combined with radiotherapy. An *in vitro* study showed that p53-deficient cancer cells are more susceptible to the combination of tepotinib and ionizing radiation (IR) (65). The results suggested that tepotinib, by inhibiting MET signaling pathway, may abolish the intra-S and G2-M checkpoint in MET-dependent cancer cells, thereby sensitize the cancer cells to DNA damage. Similar effect was demonstrated in another study investigating the combination effect of tepotinib with IR in head and neck squamous cell carcinoma both *in vitro*, *in vivo*, and *ex vivo* (66). At nanomolar concentrations, tepotinib alone did not demonstrate significant antiproliferative effect. In contrast, tepotinib, when combined with IR, was able to enhance the IR-induced G2/M cell cycle arrest, cell death and interfere the DNA repairing process.

To date, several clinical trials evaluating the anticancer effect of tepotinib were

completed or ongoing. In phase 1 clinical trials evaluating the safety and efficacy of tepotinib in patients with solid tumors, tepotinib showed relatively low toxicity and significant effect, especially in patients that overexpress MET (67-69). A phase 2 trial INSIGHT (NCT01982955) investigated the combination of tepotinib with gefitinib in NSCLC patients. The study suggested that no significant improve in progression-free survival (PFS) was found between the combination treatment (4.0 months) and chemotherapy (4.4 months) in the overall population. In addition, no benefit was demonstrated in patients harboring T790M mutation. However, the combination treatment improved the PFS in subgroups with MET overexpression or amplification (8.3 months) compared to chemotherapy (4.4 months). In particularly, over 60% of patients with MET amplification receiving combination treatment showed improved PFS, overall survival (OS), objective responses, and response duration. In another phase 2 trial VISION (NCT02864992), the efficacy and safety of tepotinib as monotherapy is under investigation in patients with advanced or metastatic NSCLC with confirmed METex14 skipping mutations (70). From the current data, tepotinib led to a partial objective response in 46% (independent review) or 56% (investigator assessment) of efficacy population with no complete response demonstrated.

In September 2019, the US FDA has granted Breakthrough Therapy Designation for tepotinib in NSCLC patients with METex14 skipping alterations who progressed following platinum-based therapy (71). The Breakthrough Therapy Designation was based on the robust, preliminary clinical data from the ongoing VISION study. In addition, in March 2020, tepotinib was approved for use in Japan for the treatment of patients with unresectable, advanced or recurrent NSCLC with METex14 skipping mutations (72). In February 2021, tepotinib was approved by the US FDA to treat NSCLC patients with METex14 skipping mutations, making it the second drug

approved after capmatinib. The recent progress achieved by tepotinib further underscores the potential of the drug, purposing it as a new focus in NSCLC treatment.

CHAPTER 2

MATERIALS AND METHODS

2.1 Chemicals and Reagents

Tepotinib was purchased from ChemieTek (Indianapolis, IN, USA). Paclitaxel, vincristine, verapamil, cisplatin, mitoxantrone, Triton X-100, 3-(4, 5-dimethylthiazol-yl)-2, 5-diphenyltetrazolium bromide (MTT) were purchased from Sigma-Aldrich (St. Louis, MO). G418, Ko143, and MK571 were products from Enzo Life Sciences (Farmingdale, NY). Cisplatin was dissolved in dimethyl formamide, all other drugs were dissolved in DMSO to a final concentration of 10 mM as stock solution. The radiolabeled drug [^{3}H]-paclitaxel and [^{3}H]-mitoxantrone were obtained from Moravek Biochemicals, Inc. (Brea, CA). Fetal bovine serum (FBS), penicillin/streptomycin, Dulbecco's modified Eagle's Medium (DMEM) and 0.25% trypsin were bought from Corning Incorporated (Corning, NY). Eagle's minimum essential medium (EMEM) was purchased from ATCC (American Type Culture Collection, Manassas, VA). Monoclonal antibodies ABCG2 (Cat #MAB4146) was purchased from Merck Millipore (Burlington, MA). Anti-mouse IgG HRP-linked antibody (Cat # 7076S) was purchased from Cell Signaling Technology Inc. (Danvers, MA). ABCB1 (Cat #MA1-26528), ABCC1 (Cat #PA5-30594), GAPDH (Cat #MA5-15738), and anti-rabbit IgG HRP-linked antibody (Cat #31460), Alexa Fluor 488-labeled anti-mouse secondary antibody (anti-mouse), 4,6-diamidino-2-phenylindole (DAPI), and other reagents were purchased from Thermo Fisher Scientific Inc. (Waltham, MA).

2.2 Cell Lines and Cell Culture

The ABCB1-overexpressing SW620/Ad300 cell line was established by selecting the human colon adenocarcinoma SW620 cell line with increasing concentration of doxorubicin (73). The SW620 and SW620/Ad300 cell lines were kind gifts from Dr. Susan E. Bates (Columbia University, NY) and Dr. Robert W. Robey (NCI, NIH, MD).

The *ABCB1* gene knockout cell lines SW620-ABCB1ko and SW620/Ad300-ABCB1ko were established by CRISPR/CRISPR-associated (Cas) 9 system (74). The ABCB1-overexpressing drug resistant cell line KB-C2 was established by introducing increasing doses of colchicine step-wise to parental human epidermoid carcinoma KB-3-1 cells (75). The ABCC1-overexpressing KB-CV60 cells were cloned from KB-3-1 cells and were maintained in medium with 1 μg/mL cepharanthine and 60 ng/mL vincristine (76). Both KB-C2, KB-CV60 and parental KB-3-1 cells were kindly provided by Dr. Shin-Ichi Akiyama (Kagoshima University, Japan). The ABCG2-overexpressing drug-resistant NCI-H460/TPT10 cells were established by exposing NCI-H460 cells to step-wise increased concentration of topotecan (77). The *ABCG2* gene knockout NCI-H460-KO and NCI-H460/TPT10-KO cell lines were constructed using CRISPR/CRISPR-associated (Cas) 9 system (77). HEK293/pcDNA3.1, HEK/ABCB1 and HEK/ABCG2 were generated by transfecting the HEK293 cells with empty pcDNA3.1 vector, *ABCB1* and *ABCG2* expressing vector accordingly (78). The ABCB1 and ABCG2 co-expressed HEK293/B1G2 cells and the parental HEK293/PEL cells were maintained in EMEM with 250 μg/mL zeocin (79). The drug-selected SW620/Ad300, KB-C2, and H460/TPT10 cells were maintained in DMEM with 300 ng/mL doxorubicin, 2 μg/mL colchicine, and 10 μM topotecan, respectively. Gene-transfected HEK293/pcDNA3.1, HEK293/ABCB1, and HEK293/ABCG2 cells were cultured in medium with 2 mg/mL G418. All cell lines were maintained in a humidified incubator at 37°C supplied with 5% CO_2. All cells were grown as an adherent monolayer and drug-resistant cells were grown in drug-free culture media for 2 weeks before assay.

2.3 Cytotoxicity Assay

The drug cytotoxicity was evaluated by the MTT colorimetric assay. Cells were

seeded evenly into 96-well plates at a density of 5×10^3 cells per well and were maintained overnight to allow cell attachment. To determine the cytotoxicity of tepotinib, different concentrations of tepotinib were added into the well. To evaluate the MDR reversal effect, serial concentrations of chemotherapeutic drugs were added into designated wells with tepotinib or positive control ABCB1 inhibitor verapamil or ABCG2 inhibitor Ko143. After 72 h of incubation, 20 μL of MTT solution (4 mg/mL) was added to each well and the cells were further incubated for additional 4 h. Then, the supernatant was discarded and replaced with 100 μL of DMSO to dissolve the formazan crystals. The AccuSkan™ GO UV/Vis Microplate Spectrophotometer (Thermo Fisher Scientific Inc., Waltham, MA, USA) was used to measure the absorbance at 570 nm. The IC50 values were calculated using the cell viability curve. The resistance-fold was calculated by dividing the IC50 value obtained from the drug-resistant cells by that from the parental cells. The concentrations of tepotinib selected for combinational treatment were below IC_{20}, where more than 80% of the cells remain viable.

2.4 [^{3}H]-substrate Accumulation and Efflux Assay

The [^{3}H]-substrate accumulation and efflux assay was performed using both parental and drug-resistant cells. For ABCB1 studies, cancer cells KB-3-1 and KB-C2 as well as gene-transfected cells HEK293/pcDNA3.1 and HEK293/ABCB1 were used. For ABCG2 studies, cancer cells NCI-H460 and NCI-H460/TPT10 as well as gene-transfected HEK293/pcDNA3.1 and HEK293/ABCG2-WT cells were used. To determine the efflux of [^{3}H]-substrate, tepotinib or positive inhibitor was added to the cells 2 h before adding 10 nM of [^{3}H]-substrate. After 2 h of incubation, cells were incubated in fresh medium with vehicle, tepotinib, or positive inhibitor. Cells were collected at different time points (0, 30, 60, 120 min) and transferred into scintillation

fluid. The radioactivity of the samples was subjected to analyze using a liquid scintillation analyzer (Packard Instrument, Downers Grove, IL, USA)

2.5 ABCB1/ABCG2 ATPase Assay

The ABCB1- and ABCG2-associated ATPase activities were measured using High-five insect cell membrane vesicle containing ABCB1 and ABCG2 transporters with modified protocols as previously described (78). Briefly, Various concentrations of tepotinib were incubated with the membranes for 5 min. The ATPase reactions were initiated by adding 5 mM Mg^{2+}-ATP. After incubating for 20 min at 37°C with brief mixing, 100 µL 5% SDS solution were added to terminate the reaction. The inorganic phosphate released during the reaction period was colorimetrically determined by spectrophotometry. The difference of inorganic phosphate level between groups were used to calculate the ATPase activity related to ABCB1 and ABCG2 transporters.

2.6 Immunofluorescence Microscopy

To perform the assay, parental and drug-resistant cells were seeded in 24-well plates at the density of 10,000 cells per well and incubated overnight (80). Subsequently, the cells were incubated with designated concentrations of tepotinib for up to 72 h. Thereafter, cells were fixed with 4% paraformaldehyde for 10 min, permeabilization with 1% Triton X-100 for 10 min and blocked with 6% BSA for 1 h at 37 ºC. The ABCB1 and ABCG2 transporters were labeled using monoclonal ABCB1 and ABCG2 antibodies (1:1000 dilution) overnight at 4 ºC, followed by incubation with Alexa flour 488 conjugated secondary antibody (1:1000 dilution) for 2 h at 37 ºC. The nuclei were stained by DAPI solution. The images were captured using an EVOS FL Auto Imaging System (Thermo Fisher Scientific Inc., Rockford, IL).

2.7 Western Blotting

Cells were treated with or without tepotinib and collected at different time points

(0, 24, 48, 72 h). Cells lysates were prepared by adding lysis buffer (25 mM Tris-HCl pH 7.6, 150 mM NaCl, 1% Triton X-100, 1% sodium deoxycholate, 0.1% SDS). Protein concentration was determined by BCA Protein Assay Kit (Thermo Scientific, Rockford, IL). Equal amounts of protein (20 μg) were subjected to sodium dodecyl sulfate polyacrylamide gel electrophoresis (SDS-PAGE) and electrophoretically transferred onto polyvinylidene fluoride (PVDF) membranes. The PVDF membranes were blocked with 5% skim milk to block non-specific binding for 2 h at room temperature. The membranes were then immunoblotted with primary monoclonal antibodies (1:1000 dilution) against GAPDH, ABCB1, or ABCG2 overnight at 4°C. Then the membrane was washed with TBST (Tris-buffered saline, 0.1% Tween 20) buffer followed by incubation for 2 h at room temperature with horseradish peroxidase (HRP)-conjugated secondary antibody (1:1000 dilution). The immunoreactive bands were developed using ECL substrate (Thermo Fisher Scientific Inc., Waltham, MA, USA) and analyzed by ImageJ software (NIH, MD, USA).

2.8 Cellular Thermal Shift Assay

The CESTA assay was performed as mentioned previously with modified protocol (81). NCI-H460/TPT10, KB-C2, and KB-CV60 cells were lysed by freezing-thawing using liquid nitrogen and 25°C heat block for five times. The protein samples were collected by centrifuging the mixture at 15,000 revolutions per minute (rpm) for 20 min. The samples were then incubated with 30 μM of tepotinib or solvent DMSO at room temperature for 30 min. Subsequently, equal amount of protein was aliquot and incubated at different temperatures from 44°C to 59°C for 3 min. Finally, the protein samples were subjected to Western blot analysis.

2.9 Molecular Docking Simulation

The docking analysis was performed in Maestro v11.1 (Schrödinger, LLC) as

described previously (82). The protein was prepared and the docking grid at drug-binding pocket of human ABCB1 model (PDB: 6FN1) (83) and human ABCG2 model (PDB: 6FFC) (29) was generated by the default protocol. Ligand preparation of tepotinib was essentially performed. Glide XP docking was performed, and then induced-fit docking was conducted with the default protocol. The top-scoring pose (sorted by affinity score: kcal/mol) was selected for further analysis and visualization.

2.10 Experimental Animals

Male athymic NCR nude mice (18-23 g, 5 weeks old) were obtained from the Taconic Farms (Albany, NY). The animal study was reviewed and approved by the Institutional Animal Care and Use Committee of St. John's University (Protocol #1962), and the project was conducted in compliance with the Animal Welfare Act and other federal statutes. The animals were kept under alternate light/dark cycles, provided with food and water, and kept in polycarbonate cages (4 mice/cage). The mice were housed at the St. John's University Animal Care Center and were regularly examined for tumor growth by measuring the size using Vernier calipers.

2.11 Tumor Xenograft Model

To establish the xenograft models, $3\text{-}5 \times 10^6$ of NCI-H460 or NCI-H460/TPT10 cells were injected subcutaneously under the armpits of the mice. When the tumors reached a palpable volume, the mice were separated into four groups (n=6) and treated with one of the following regimens every 3rd day for a total of 6 times: (1) vehicle (5% DMSO + 30% PEG 300 +10% Tween-20 + 55% Normal saline, p.o.); (2) tepotinib diluted in vehicle solution (30 mg/kg, p.o.); (3) topotecan diluted in normal saline (3.0 mg/kg, i.p.) and (4) combination of topotecan (3.0 mg/kg, i.p.) and tepotinib (30 mg/kg, p.o.). At the end of the study, the mice were euthanized by carbon dioxide, and the tumors were excised and weighed. Tumor volumes (V) and the ratio of growth

inhibition (IR) for tumor weight (IRW) and tumor volume (IRV) were calculated using the equations given below:

$$V = \frac{\pi}{6} \left(\frac{A + B}{2} \right)^3$$

$$IRW(\%) = \left(1 - \frac{mean\ tumor\ weight\ of\ treatment\ group}{mean\ tumor\ weight\ of\ vehicle\ group} \right) \times 100$$

$$IRV(\%) = \left(1 - \frac{mean\ tumor\ volume\ of\ treatment\ group}{mean\ tumor\ volume\ of\ vehicle\ group} \right) \times 100$$

2.12 Collection of Plasma and Tumor Sample

The tumor samples were homogenized using 10 mL PBS. The homogenized mixture was extracted with 10 mL diethyl ether. The mixture was centrifuged at 4⁰C at 1,500 rpm for 10 min and then the diethyl ether layer was collected. The solvent was evaporated, and the residue was redissolved in 500 mL methanol: TFA (10:1) mixture. For the plasma samples, 500 mL methanol: TFA (10:1) mixture was added. Subsequently, both plasma and tumor samples were kept on ice for 30 min to allow protein precipitation. It was then centrifuged at 15,000 rpm at 4⁰C for 20 min. The supernatant was collected and filtered through 0.2 mm filter into HPLC vials and then the samples were analyzed using HPLC.

2.13 HPLC Analysis Method

The Agilent 1260 infinity series was used to analyze the samples. The Agilent C18 column with dimensions 5 mm x 250 x 4.6 mm was used. The solvent system used was A= water (with 0.1% formic acid) and B= acetonitrile (with 0.1% formic acid). The injection volume used was 100 mL and the detector wavelength used was 254 nm. LR-LC/MS analyses were performed on single quadrupole Agilent Technologies 1260 infinity series LC. The following method was used for verifying exact masses of compounds: Column = Agilent Poroshell 120 EC-C18 2.7 μm, 4.6 x 50 mm.; temperature = 300 K; solvent acetonitrile/water 70:30 (0.1% formic acid): flow rate 0.5

mL/min; isocratic; 25 µL injection and each single run lasted for 5 min.

2.14 Statistical Analysis

All calculation and statistical analyses were performed in GraphPad software (Prism 7.0). Data were expressed as the mean ± standard deviations (SD). Statistical analysis was performed using a one-way ANOVA and a P value < 0.05 was considered statistically significant.

CHAPTER 3

RESULTS

3.1 The Cytotoxicity of Tepotinib was Not Affected by MDR-related ABC Transporters

The cytotoxicity profile of tepotinib was first obtained from parental and drug-resistant cells to determine if it is a substrate of MDR-related ABC transporters. The cells were treated with tepotinib (0-100 μM) for 72 h and the cell viability was determined using MTT assay. As shown in **Fig.1**, both ABCB1-overexpressing cancer cells SW620/Ad300 and KB-C2 showed similar response to tepotinib as the parental SW620 and KB-3-1 cells. In **Fig.2**, tepotinib had identical cytotoxicity in ABCG2-overexpressing NCI-H460/TPT10 cells and ABCC1-overexpressing KB-CV60 cells as compared with the parental NCI-H460 and KB-3-1 cells, respectively. Moreover, the observation was confirmed in HEK293 cells transfected with *ABCB1* or *ABCG2* genes. Therefore, the results showed that the efficacy of tepotinib is not affected by the three MDR-related ABCB1, ABCG2, and ABCC1 transporter. The maximum non-toxic concentration is 3 μM based on the cell viability curves and can be equally reached in both parental and drug-resistant cells. Therefore, based on these results, the non-toxic concentrations (0.1-3 μM) of tepotinib were chosen to minimize cytotoxicity in the tepotinib-substrate drug combination experiments.
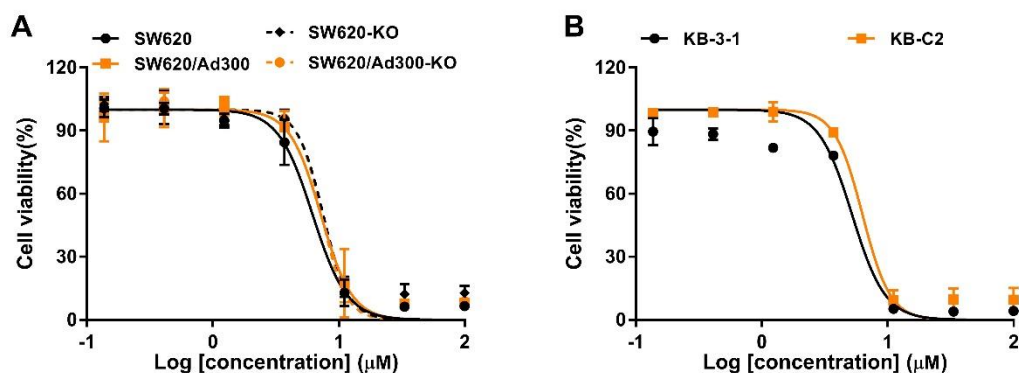
Figure 1. Cytotoxicity of tepotinib in parental and ABCB1-overexpressing cells. (**A**) Cell viability curves for SW620, SW620/Ad300, and *ABCB1* gene knockout cells. (**B**) Cell viability curves for KB-3-1 and KB-C2 cells. Data are expressed as mean ± SD from a representative of three independent experiments (n=3).
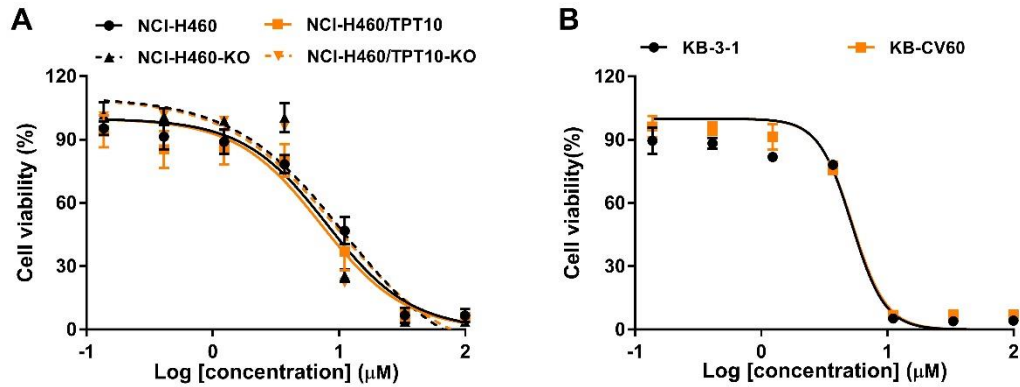
Figure 2. Cytotoxicity of tepotinib in parental and ABCG2- and ABCC1-overexpressing cells. (**A**) Cell viability curves for NCI-H460, NCI-H460/TPT10, and *ABCG2* gene knockout cells. (**B**) Cell viability curves for KB-3-1 and KB-CV60 cells. Data are expressed as mean ± SD from a representative of three independent experiments (n=3).
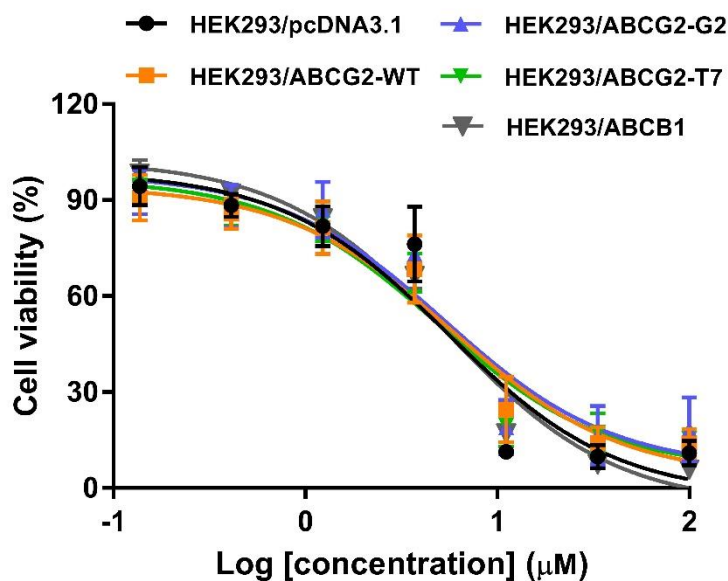
Figure 3. Cytotoxicity of tepotinib in HEK293 cells. Cell viability curves for HEK293 transfected with empty vector pcDNA3.1, ABCB1, wild-type and mutant ABCG2 gene. Data are expressed as mean $\pm$ SD from a representative of three independent experiments (n=3).

3.2 Tepotinib Sensitized ABCB1-Overexpressing Cells to ABCB1 Substrate Drugs

To evaluate the MDR reversal effect, parental SW620 and ABCB1-overexpressing SW620/Ad300 cancer cells were incubated with tepotinib plus ABCB1 substrate drugs paclitaxel or vincristine. As shown in **Table.1**, Compared to the parental SW620 cells, drug-resistant SW620/Ad300 cells showed significant resistance to substrate drugs paclitaxel (45-fold) and vincristine (38-fold) due to the overexpression of ABCB1 transporter. Tepotinib significantly sensitized drug-resistant SW620/Ad300 cells to substrate drugs paclitaxel and vincristine in a concentration-dependent manner without affecting the treatment response in parental SW620 cells. At 0.3 μM, tepotinib completely reversed the drug resistance to paclitaxel and vincristine in drug-resistant SW620/Ad300 cells. And 0.1 μM of tepotinib was able to decrease the resistance-fold (RF) of paclitaxel and vincristine to 7.4- and 5.8-fold, respectively. Compared to the positive ABCB1 inhibitor verapamil, tepotinib may have a stronger reversal effect at low concentrations. When *ABCB1* gene was knockout from both parental SW620 and drug-resistant SW620/Ad300 cells, the IC$_{50}$ values of paclitaxel and vincristine in SW620-KO and SW620/Ad300-KO cells are similar to that in parental SW620 cells. Importantly, the MDR reversal effect of tepotinib was abolished in *ABCB1* gene knockout cells, suggesting tepotinib may interact with ABCB1 to reverse drug resistance.

Subsequently, the MDR reversal effect was validated in gene transfected HEK293

cells using 0.3 and 0.1 µM of tepotinib. The transfection of HEK293 cells with the *ABCB1* gene significantly decreased the efficacy of paclitaxel (RF = 70.5) and vincristine (RF = 60.8) compared to HEK293 cells transfected with an empty pcDNA3.1 vector (**Table.2**). The incubation of HEK293/ABCB1 cells with tepotinib or verapamil significantly decreased the RF of paclitaxel and vincristine. Tepotinib at 0.1 µM showed a partial reversal effect in HEK/ABCB1 cells. While verapamil required 3 µM to achieve reversal effect, 0.3 µM of tepotinib was able to significantly sensitize HEK293/ABCB1 to both paclitaxel and vincristine, and the reversal effect was comparable to 3 µM of verapamil.

Table 1. Tepotinib reverses ABCB1-mediated MDR in drug-resistant cancer cells

Treatment	IC50 mean ± SD (µM, Resistance folda)			
	SW620	SW620/Ad300	SW620-KO	SW620/Ad300-KO
Paclitaxel	0.057±0.032	2.552±0.249	0.053±0.014	0.054±0.008
	(1.00)	(44.54) *	(0.93)	(0.94)
+ Tepotinib	0.068±0.041	0.422±0.033	0.064±0.029	0.046±0.011
0.1 µM	(1.18)	(7.37)	(1.12)	(0.81)
+ Tepotinib	0.072±0.035	0.280±0.015	0.048±0.016	0.048±0.029
0.3 µM	(1.26)	(4.89)	(0.84)	(0.84)
+ Verapamil	0.072±0.044	0.318±0.016	0.046±0.007	0.058±0.008
0.3 µM	(1.25)	(5.55)	(0.80)	(1.01)
Vincristine	0.044±0.003	1.691±0.612	0.044±0.014	0.043±0.014
	(1.00)	(38.04) *	(0.99)	(0.97)

+ Tepotinib	0.051±0.007	0.257±0.055	0.035±0.010	0.042±0.012
0.1 μM	(1.15)	(5.78)	(0.79)	(0.95)
+ Tepotinib	0.040±0.005	0.173±0.024	0.033±0.010	0.038±0.019
0.3 μM	(0.89)	(3.90)	(0.74)	(0.86)
+ Verapamil	0.042±0.011	0.295±0.027	0.037±0.016	0.035±0.005
0.3 μM	(0.95)	(6.64)	(0.83)	(0.79)

Data are shown as mean ± SD from three independent experiments (n=3).

a Rf: Resistance fold was calculated by dividing the IC50 values of substrates in the presence or absence of inhibitor by the IC50 of SW620 cells without inhibitor.

* $P < 0.05$ versus the control group without inhibitor

Table 2. Tepotinib reverses ABCB1-mediated MDR in ABCB1-transfected cells

Treatment	IC_{50} mean ± SD (μM, Resistance fold[a])	
	HEK293/pcDNA3.1	HEK293/ABCB1
Paclitaxel	0.013 ± 0.006 (1.0)	0.933 ± 0.441 (70.5)
+ Tepotinib 0.1 μM	0.011 ± 0.007 (0.8)	0.484 ± 0.270 (36.6)
+ Tepotinib 0.3 μM	0.008 ± 0.005 (0.6)	0.095 ± 0.045* (7.2)
+ Verapamil 0.3 μM	0.010 ± 0.008 (0.7)	0.546 ± 0.364 (41.3)
+ Verapamil 3 μM	0.012 ± 0.001 (0.9)	0.062 ± 0.039* (4.7)
Vincristine	0.005 ± 0.002 (1.0)	0.328 ± 0.066 (60.8)
+ Tepotinib 0.1 μM	0.005 ± 0.004 (1.0)	0.187 ± 0.065 (34.7)
+ Tepotinib 0.3 μM	0.006 ± 0.001 (1.1)	0.043 ± 0.026* (8.1)
+ Verapamil 0.3 μM	0.005 ± 0.002 (0.9)	0.202 ± 0.134 (37.4)

+ Verapamil 3 µM	0.006 ± 0.001 (1.1)	0.016± 0.009* (3.0)

Data are shown as mean ± SD from three independent experiments (n=3).

[a] Rf: Resistance fold was calculated by dividing the IC_{50} values of substrates in the presence or absence of inhibitor by the IC_{50} of HEK293/pcDNA3.1 cells without inhibitor.

* $P < 0.05$ versus the control group without inhibitor

3.3 Tepotinib Sensitized ABCG2-Overexpressing Cells to ABCG2 Substrate Drugs

Based on the cytotoxicity results, 1 and 3 µM of tepotinib, which did not significantly affect to cell viability, were selected to conduct the ABCG2 MDR reversal studies. As shown in **Table.3**, NCI-H460/TPT10 cells were significantly resistant to mitoxantrone (92-fold) and topotecan (168-fold) as compared to the parental NCI-H460 cells. In the combinational treatment, 1 and 3 µM of tepotinib enhanced the cytotoxicity and decreased the resistance fold of mitoxantrone (12- and 3-fold) and topotecan (27- and 4-fold) in drug-resistant NCI-H460/TPT10 cells without affecting to the parental NCI-H460 cells. In addition, the reversal effect of tepotinib at 3 µM was comparable to that of the positive ABCG2 inhibitor Ko143. When the *ABCG2* gene was knockout from the drug-resistant NCI-H460/TPT10 cells, the cells became sensitive to mitoxantrone and topotecan. Importantly, the MDR reversal effect of tepotinib was not observed in the NCI-H460/TPT10-KO cells.

It has been shown that mutations at residue 482 in the ABCG2 transporter can affect the substrate transport profile and the efficacy of reversal inhibitors. Therefore, we further examined the reversal effect of tepotinib in HEK293 cells overexpressing wild-type (WT) or mutant ABCG2 transporter. As shown in **Table.4**, similar to the observation in drug-resistant cancer cells, the sensitizing effect was demonstrated in

HEK293/ABCG2-WT as well as R482G and R482T mutant cells. The transfection of HEK293 cells with the genes coding for the ABCG2-WT, ABCG2-R482G, and ABCG2-R482T mutant proteins, significantly decreased the efficacy of mitoxantrone and topotecan compared to HEK293 cells transfected with an empty pcDNA3.1 vector (**Table.4**). Moreover, similar to the observation in drug-resistant cancer cells, the sensitizing effect was demonstrated in HEK293/ABCG2-WT as well as R482G and R482T mutant cells. In the ABCB1/ABCG2 double-transfected HEK293/B1G2 cells, tepotinib was able to significantly decrease the resistance fold of doxorubicin (from 45-fold to 3.6-fold). Moreover, as shown in **Fig.4**, the reversal effect of tepotinib is stronger than verapamil, a known ABCB1 inhibitor (from 45-fold to 6.6-fold) or ABCG2 inhibitor Ko143 (from 45-fold to 9.4-fold), suggesting tepotinib may serve as dual ABCB1/ABCG2 reversal inhibitor.

Table 3. Tepotinib reverses ABCG2-mediated MDR in drug-resistant cancer cells

Treatment	IC_{50} mean $\pm$ SD (μM, Resistance fold[a])			
	NCI-H460	NCI-H460/TPT10	NCI-H460-KO	NCI-H460/TPT10-KO
Mitoxantrone	0.016 ± 0.007	1.472 ± 0.270	0.010 ± 0.001	0.012 ± 0.003
	(1.00)	(92.0) [*]	(0.63)	(0.75)
+ Tepotinib	0.017 ± 0.001	0.190 ± 0.059	0.009 ± 0.002	0.009 ± 0.002
1 μM	(1.06)	(11.88) [*]	(0.56)	(0.56)
+ Tepotinib	0.013 ± 0.005	0.059 ± 0.003	0.010 ± 0.003	0.009 ± 0.002
3 μM	(0.81)	(3.69)	(0.63)	(0.56)
+ Ko143	0.019 ± 0.012	0.040 ± 0.007	0.010 ± 0.002	0.009 ± 0.003

3 μM	(1.4)	(2.50)	(0.56)	(0.56)
Topotecan	0.090 ± 0.011	15.12 ± 0.953	0.070 ± 0.004	0.072 ± 0.008
	(1.00)	(168.00)[*]	(0.78)	(0.80)
+ Tepotinib	0.122 ± 0.026	2.416 ± 0.128	0.081 ± 0.003	0.078 ± 0.007
1 μM	(1.36)	(26.84)[*]	(0.90)	(0.87)
+ Tepotinib	0.090 ± 0.032	0.393 ± 0.179	0.070 ± 0.009	0.076 ± 0.007
3 μM	(1.00)	(4.37)	(0.78)	(0.84)
+ Ko143	0.089 ± 0.030	0.534 ± 0.125	0.065 ± 0.005	0.065 ± 0.007
3 μM	(0.99)	(5.93)	(0.72)	(0.73)

Data are shown as mean $\pm$ SD from three independent experiments (n=3).

[a] Rf: Resistance fold was calculated by dividing the IC_{50} values of substrates in the presence or absence of inhibitor by the IC_{50} of NCI-H460 cells without inhibitor.

* $P < 0.05$ versus the control group without inhibitor

Table 4. Tepotinib reverses ABCG2-mediated MDR in gene-transfected HEK293 cells

Treatment	IC_{50} mean $\pm$ SD (μM, Resistance fold[a])			
	pcDNA3.1	ABCG2-WT	ABCG2-R482G	ABCG2-R482T
Mitoxantrone	0.020 ± 0.003	0.522 ± 0.050	0.719 ± 0.159	1.508 ± 0.318
	(1.00)	(26.10)[*]	(35.95)[*]	(75.40)[*]
+ Tepotinib 1 μM	0.021 ± 0.009	0.065 ± 0.021	0.086 ± 0.009	0.056 ± 0.021
	(1.05)	(3.25)	(4.3)	(2.80)
+ Tepotinib 3 μM	0.022 ± 0.005	0.018 ± 0.006	0.037 ± 0.002	0.023 ± 0.004
	(1.10)	(0.90)	(1.85)	(1.15)

+ Ko143 3 µM	0.015 ± 0.010 (0.75)	0.021 ± 0.008 (1.05)	0.039 ± 0.005 (1.95)	0.028 ± 0.015 (1.40)
Topotecan	0.133 ± 0.006 (1.00)	3.307 ± 1.109 (24.86) [*]	2.419 ± 0.742 (18.19) [*]	8.274 ± 1.865 (62.21) [*]
+ Tepotinib 1 µM	0.131 ± 0.070 (0.98)	0.460 ± 0.216 (3.46)	0.553 ± 0.058 (4.16)	1.390 ± 0.518 (10.45) [*]
+ Tepotinib 3 µM	0.125 ± 0.067 (0.94)	0.329 ± 0.152 (2.47)	0.287 ± 0.152 (2.16)	0.603 ± 0.331 (4.53)
+ Ko143 3 µM	0.134 ± 0.039 (1.01)	0.400 ± 0.221 (3.01)	0.205 ± 0.102 (1.54)	0.227 ± 0.067 (1.71)

Data are shown as mean ± SD from three independent experiments (n=3).

[a] Rf: Resistance fold was calculated by dividing the IC_{50} values of substrates in the presence or absence of inhibitor by the IC_{50} of HEK293/pcDNA3.1 cells without inhibitor

* $P < 0.05$ versus the control group without inhibitor

Figure 4. The effects of tepotinib on the cytotoxicity of doxorubicin in parental HEK293/pcDNA3.1 and ABCB1/ABCG2 co-expressed HEK293/B1G2 cell. Data are expressed as mean $\pm$ SD from a representative of three independent experiments (n=3). *$p < 0.05$ versus the corresponding control group.

3.4 Tepotinib Did Not Affect the Cytotoxicity of Non-substrate Drug Cisplatin

To confirm the MDR reversal effect of tepotinib is related to ABC transporters, cisplatin was used as negative control. Cisplatin, a non-substrate drug, showed similar cytotoxicity in parental and MDR cancer cells. As shown in **Fig.5A**, the treatment of cisplatin combined with tepotinib or verapamil did not affect the cytotoxicity of cisplatin in parental SW620 and drug-resistant SW620/Ad300 cells. Similarly, tepotinib or Ko143 did not affect the cytotoxicity of cisplatin in parental NCI-H460 and drug-resistant NCI-H460/TPT10 cells (**Fig.5B**). Finally, as expected, neither tepotinib nor positive inhibitors significantly altered the IC_{50} values of the cisplatin in HEK293 cells transfected with *ABCB1* or *ABCG2* gene (**Fig.6**).
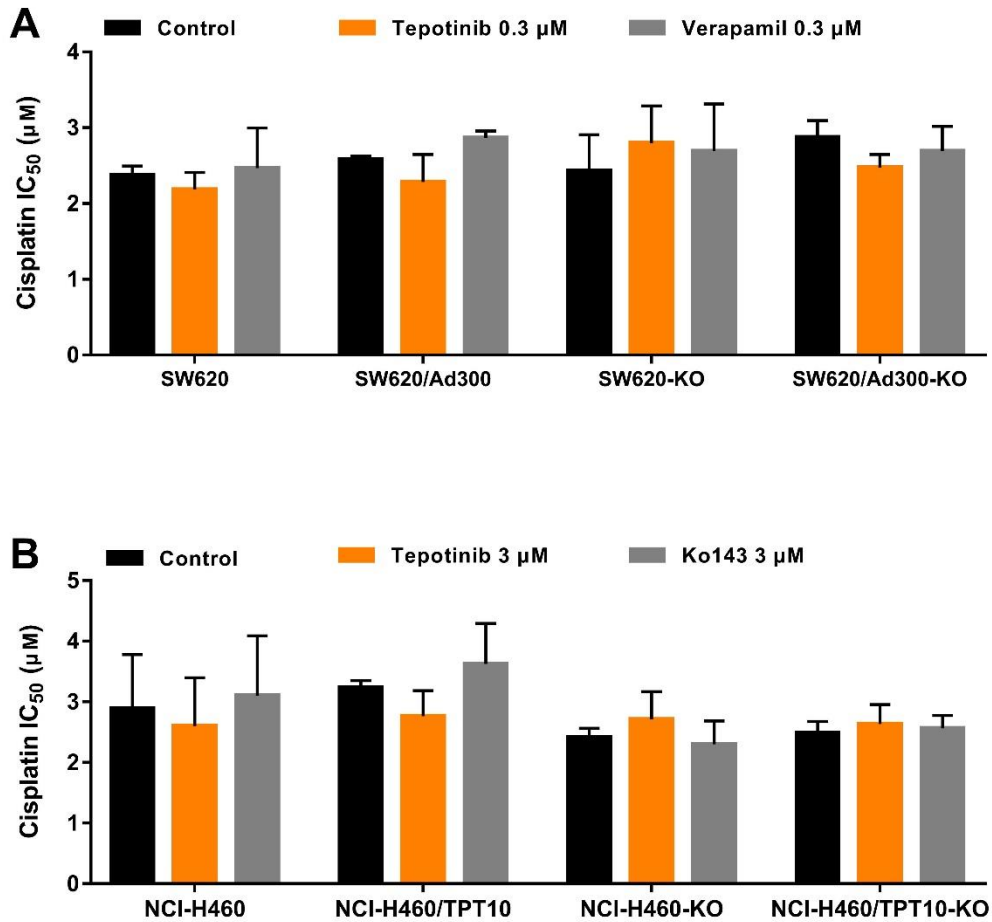
Figure 5. The effects of tepotinib on the cytotoxicity of cisplatin in parental and drug-resistant cancer cells. (**A**) parental and ABCB1-overexpressing cancer cells, (**B**) parental and ABCG2-overexpressing cancer cells. Data are expressed as mean $\pm$ SD from a representative of three independent experiments (n=3). *$p < 0.05$ versus the corresponding control group.
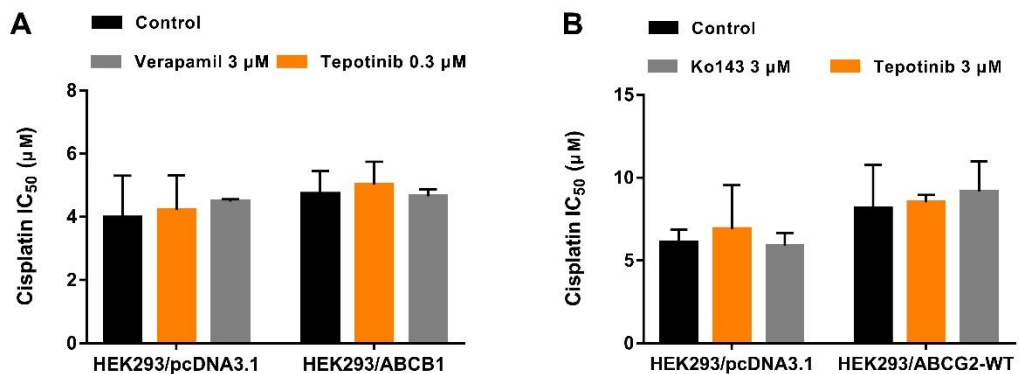
Figure 6. The effects of tepotinib on the cytotoxicity of cisplatin in gene-transfected HEK293 cells. (**A**) parental HEK293/pcDNA3.1 and ABCB1-overexpressing HEK/ABCB1 cells, (**B**) parental HEK293/pcDNA3.1 and ABCG2-overexpressing HEK/ABCG2-WT cells. Data are expressed as mean ± SD from a representative of three independent experiments (n=3). *p < 0.05 versus the corresponding control group.

3.5 Western Blot Assay

It is possible that the MDR reversal effect of tepotinib in the drug-resistant cancer cells could be due to downregulating the expression level of ABCB1/ABCG2 transporters. Therefore, we performed Western blot analysis to evaluate the effect of tepotinib on ABCB1/ABCG2 protein expression level. As shown in **Fig.7A**, while the parental KB-3-1 cells had no ABCB1 expression, KB-C2 cells showed a high expression of ABCB1 protein, confirming its ABCB1-overexpressing phenotype. The incubation of KB-C2 cells with 0.3 μM of tepotinib for up to 72 h did not alter the expression level of ABCB1 compared to control group. As shown in **Fig.7B**, the NCI-H460 cells had low endogenous ABCG2 level and NCI-H460/TPT10 cells exhibited high ABCG2 expression. Tepotinib, at 3 μM, did not affect ABCG2 expression throughout the 72 h incubation period compared to the control. Therefore, it is unlikely that tepotinib can cause ABCB1/ABCG2 protein downregulation.
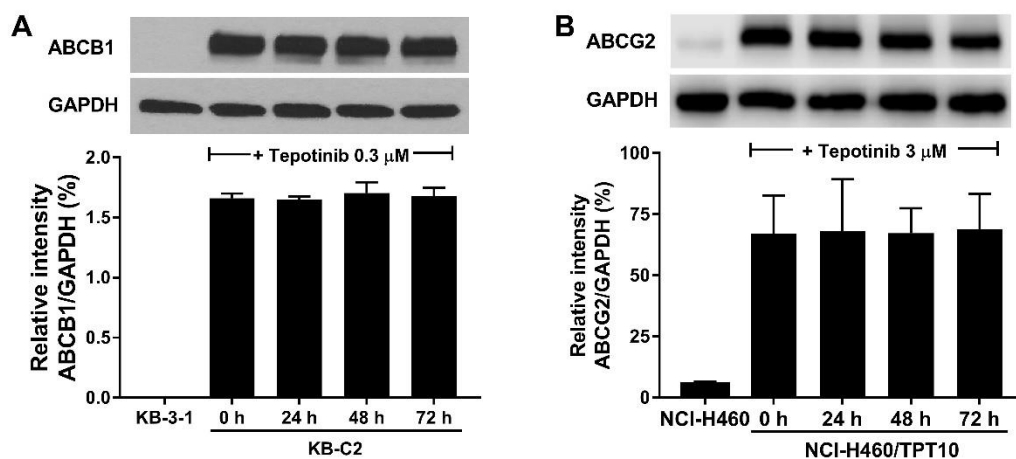
Figure 7. The effects of tepotinib on ABCB1 and ABCG2 protein expression level in drug-resistant cancer cells. (**A**) ABCB1-overexpressing KB-C2 cells, (**B**) ABCG2-overexpressing NCI-H460/TPT10 cells. Data are expressed as mean $\pm$ SD from three independent experiments (n=3). *$p < 0.05$ versus the corresponding control group.

3.6 Immunofluorescence Assay

An alteration in the membrane localization of the ABCB1/ABCG2 transporters (i.e., the transporters would not be located in the cell membrane and thus cannot efflux the substrate drugs from the drug-resistant cancer cells) could decrease the resistance to the anticancer drugs. Consequently, we used an immunofluorescence assay to determine if tepotinib altered the membrane localization of the ABCB1 and ABCG2 transporters in drug-resistant KB-C2 and NCI-H460/TPT10 cancer cells, respectively. As shown in **Fig.8**, the ABCB1 transporter in KB-C2 cells is mainly expressed on cell membrane as indicated by the enriched green fluorescence. Incubation of KB-C2 cells with 0.3 μM of tepotinib for 24, 48, or 72 h did not affect to the localization of ABCB1 after 72 h. Similarly, in **Fig.9**, the results showed that tepotinib did not cause ABCG2 transporter internalization after 72 h treatment. These data suggest that the MDR reversal effect of tepotinib in drug-resistant cells is not due to an alteration in the

membrane localization of the ABCB1/ABCG2 transporters.
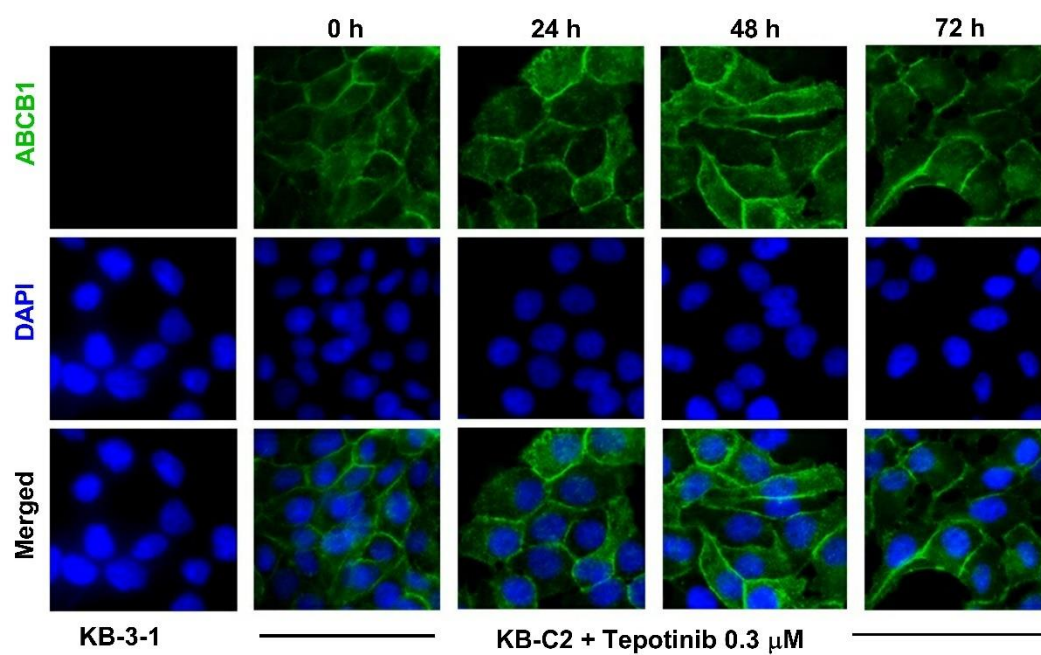
Figure 8. The effects of tepotinib on ABCB1 membrane localization in parental KB-3-1 and ABCB1-overexpressing KB-C2 cells.
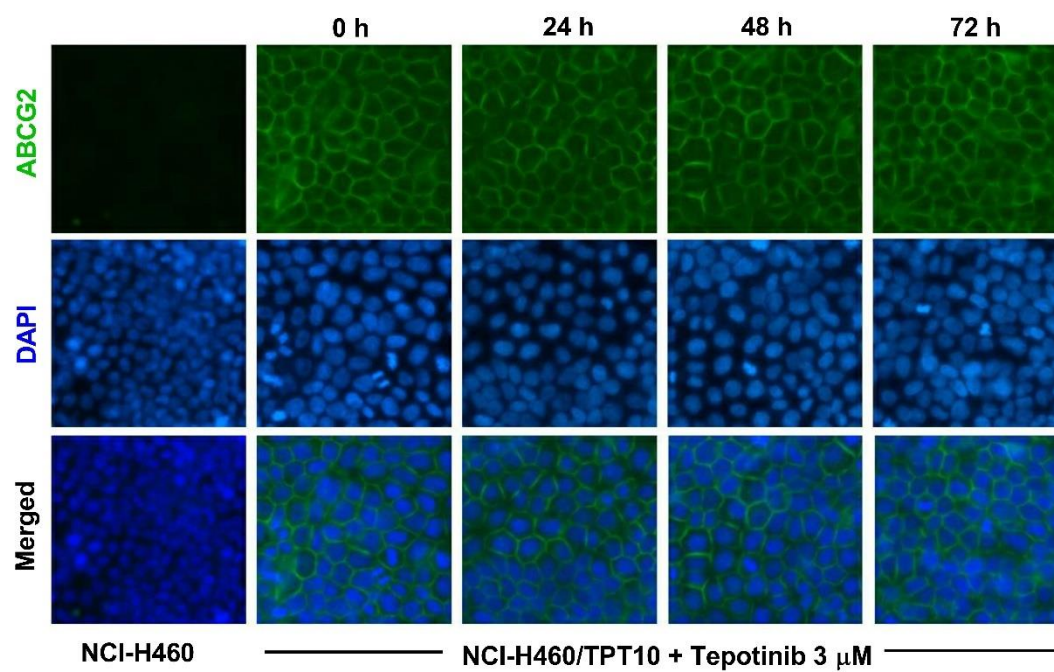
Figure 9. The effects of tepotinib on ABCG2 membrane localization in parental NCI-H460 and ABCG2-overexpressing NCI-H460/TPT10 cells.

3.7 Cellular Thermal Shift Assay

The CESTA assay was conducted to confirm the binding of tepotinib with ABC transporters. It is proposed that, upon heating, the target protein will unfold and precipitate, while a ligand engaged protein will require a higher temperature to unfold and precipitate. As shown in **Fig.10,** tepotinib treatment can stabilize ABCB1 and ABCG2 protein against high temperatures compared to the solvent control DMSO. In the solvent control group, both ABCB1 and ABCG2 protein signal decreased in a temperature-dependent manner from 50°C to 59°C. When tepotinib was incubated with the protein samples, it increased ABCB1 and ABCG2 thermal stability as demonstrated by the unaffected protein band density, suggesting a direct binding interaction between tepotinib and the transporters. In contrast, tepotinib did not affect to the thermal profile of ABCC1 (negative control).
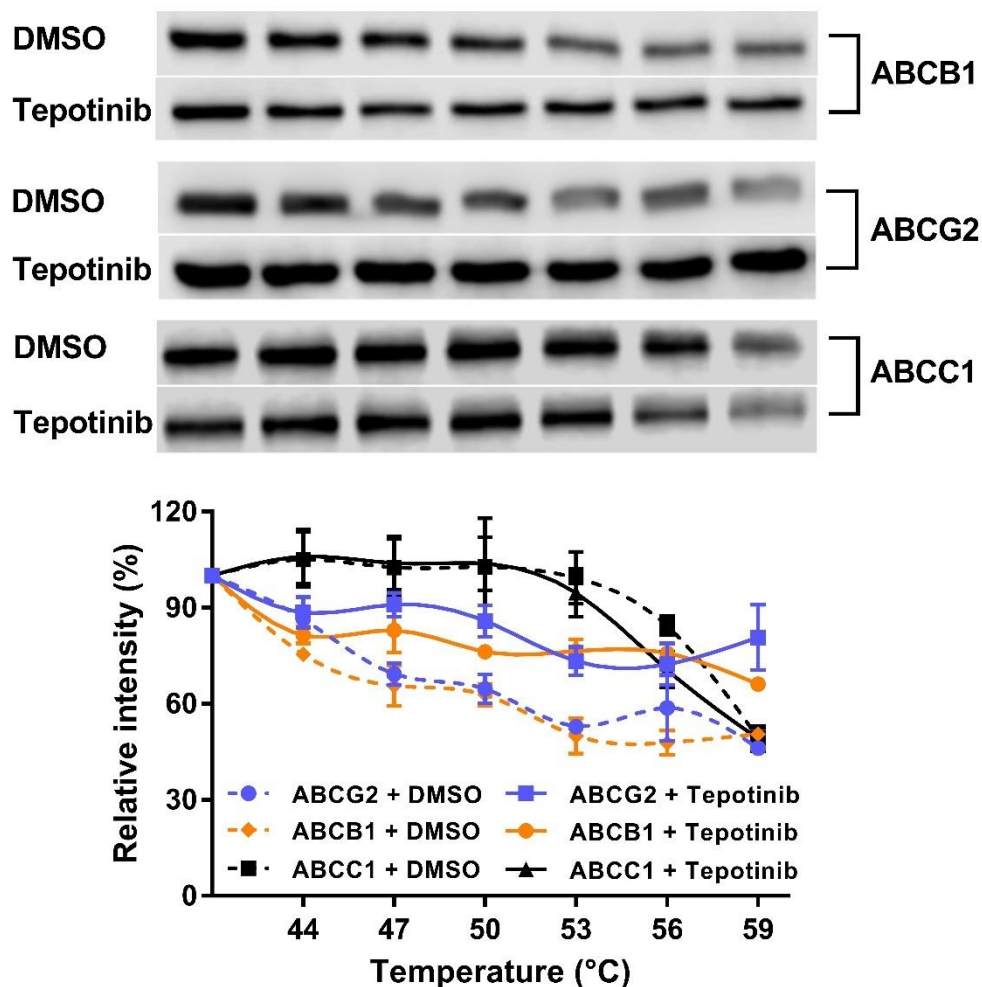
Figure 10. Cellular thermal shift assay melting curve of ABCG2/ABCB1/ABCC1. The protein was incubated with DMSO or 30 μM of tepotinib followed by different temperature for 3 min. Data are expressed as mean ± SD from three independent experiments (n=3). *$p < 0.05$ versus the control group.

3.8 ATPase Assay

ATPase assay was conducted to further validate whether tepotinib has direct interaction with ABCB1 and ABCG2 transporters. It is suggested that certain reversal inhibitors can either inhibit or stimulate the ABCB1/ABCG2 ATPase. As shown in **Fig.11A**, tepotinib, in 0-5 μM range, inhibited the ATPase activity of ABCB1 at a

concentration-dependent manner while paclitaxel, a substrate of ABCB1, stimulated the ATPase activity. The concentration of tepotinib required to obtain 50% of maximal inhibition was 0.53 μM and the maximum inhibition was 0.02-fold compared to basal activity. Paclitaxel stimulated the ATPase activity of ABCB1 with a maximal stimulation of 2.75-fold of the basal activity and 0.03 μM of tepotinib was able to completely inhibit the ATPase activity stimulated by paclitaxel. These results indicated that tepotinib may inhibit the ATPase activity of ABCB1, thereby limiting the energy released from ATP hydrolysis. According to the results presented in **Fig.11B**, tepotinib, in 0-40 μM range, stimulated ABCG2 ATPase in a concentration-dependently manner with a maximum 7.6-fold stimulation at 20 μM. The stimulatory effect of tepotinib reached EC_{50} at 1.23 μM, which falls within the reversal concentrations used in the ABCG2 study. Therefore, tepotinib may bind to the substrate-binding site of ABCG2 transporter and stimulate the function of ABCG2 ATPase. The alteration of the ABCG2 and ABCB1 transporter ATPase activity by tepotinib suggests that it may exhibit different binding interaction with ABCB1 and ABCG2 transporters.
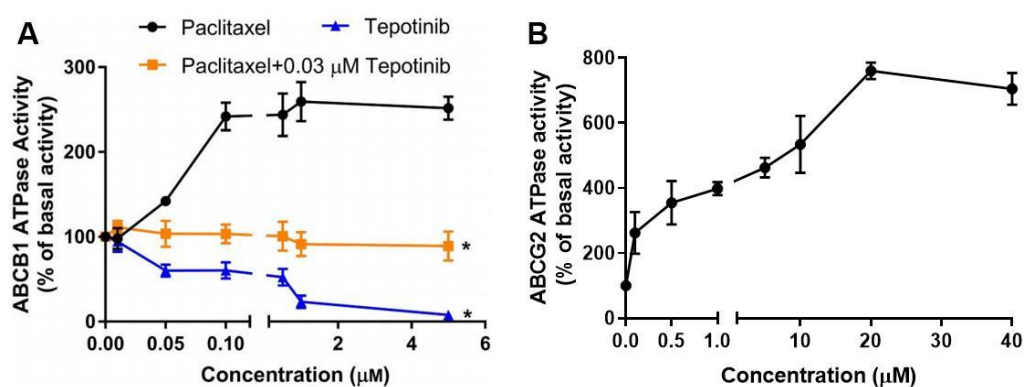

Figure 11. The effects of tepotinib on vanadate (Vi)-sensitive ABCB1/ABCG2 ATPase activity. (**A**) The effect of tepotinib (0-5 μM) on ABCB1 ATPase activity. Paclitaxel is an ABCB1 substrate that can stimulate ABCB1 ATPase activity. (**B**) The effect of tepotinib (0-40 μM) on ABCG2 ATPase activity. Data are expressed as mean ± SD from

three independent experiments (n=3). *p < 0.05 versus the corresponding control group.

3.9 Tepotinib Increased [³H]-Substrate Accumulation in MDR Cells

The MDR reversal effect of tepotinib may be due to increasing the substrate drug accumulation in drug-resistant cells. Therefore, two pairs of cancer cells were used to explore this mechanism and gene-transfected HEK293 cells were used as validation. The substrate accumulation and efflux profiles in drug-resistant cells were determined using [³H]-paclitaxel and [³H]-mitoxantrone, which are substrates for ABCB1 and ABCG2 transporters, respectively. As shown in **Fig.12**, the intracellular level of [³H]-paclitaxel was significantly downregulated in ABCB1-overexpressing KB-C2 cells than parental KB-3-1 cells, suggesting a large portion of paclitaxel was removed from the drug-resistant cells. Tepotinib increased the accumulation of [³H]-paclitaxel in the drug-resistant KB-C2 cells but not in parental KB-3-1 cells. At 0.3 μM, tepotinib showed a stronger effect than the positive inhibitor verapamil. The similar result was observed in gene-transfected cells that 0.3 μM of tepotinib significantly increased the accumulation of [³H]-paclitaxel in HEK293/ABCB1 cells without affecting that in the HEK293/pcDNA3.1 cells.

In ABCG2-overexpressing NCI-H460/TPT10 cells (**Fig.13**), the vehicle-treated cells demonstrated active drug efflux process as indicated by the decreased intracellular [³H]-mitoxantrone accumulation. The incubation of drug-resistant cells with either tepotinib or Ko143 significantly upregulated the intracellular level of [³H]-mitoxantrone following 2 h of incubation with tepotinib or Ko143. At 3 μM, tepotinib restored the mitoxantrone accumulation level in drug-resistant NCI-H460/TPT10 cells to the similar extent observed in the parental NCI-H460 cells. In contrast, [³H]-mitoxantrone accumulation level was not significantly altered by incubation with either

tepotinib (1 or 3 μM) or Ko143 (3 μM) in the parental NCI-H460 cells which do not overexpress the ABCG2 transporter.
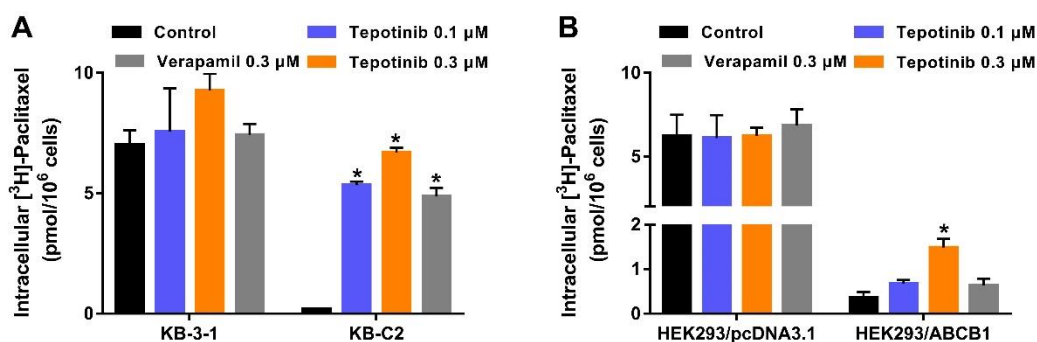
Figure 12. The effects of tepotinib on the accumulation of [³H]- paclitaxel in ABCB1-overexpressing cells. (**A**) The accumulation of [³H]-paclitaxel in KB-3-1 and KB-C2 cells. (**B**) The accumulation of [³H]-paclitaxel in HEK293/pcDNA3.1 and HEK293/ABCB1 cells. Data are expressed as mean ± SD from three independent experiments (n=3). *$p < 0.05$ versus the control group.
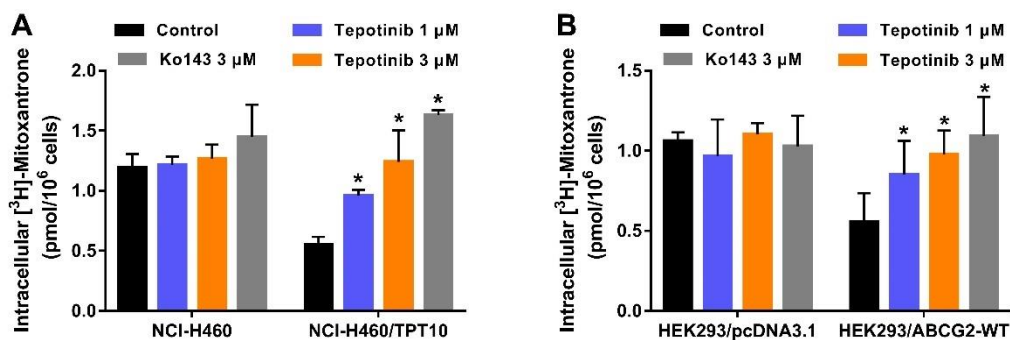
**Figure 13.** The effects of tepotinib on the accumulation of [³H]-mitoxantrone in ABCG2-overexpressing cells. (**A**) The accumulation of [³H]-mitoxantrone in NCI-H460 and NCI-H460/TPT10 cells. (**B**) The accumulation of [³H]-mitoxantrone in HEK293/pcDNA3.1 and HEK293/ABCG2-WT cells. Data are expressed as mean ± SD from three independent experiments (n=3). *$p < 0.05$ versus the control group.

3.10 Tepotinib Inhibited [^{3}H]-Substrate Efflux in MDR Cells

Because increasing substrate accumulation can be attributed to increased substrate influx and/or decreased substrate efflux, [^{3}H]-substrate efflux assay was performed to investigate this factor using both drug-resistant cancer cells and gene-transfected HEK293 cells. As shown in **Fig.14A and C**, tepotinib did not affect the drug efflux process in parental KB-3-1 or HEK293/pcDNA3.1 cells. In contrast, both drug-resistant cells demonstrated a significant decrease of intracellular [^{3}H]-paclitaxel, from 100% to 10%. However, treatment with tepotinib significantly inhibited the efflux activity in drug-resistant KB-C2 and HEK293/ABCB1 cells (**Fig14.B and D**). The intracellular [^{3}H]-paclitaxel increased from 10% to 60% in KB-C2 cells, and from 10% to 30% in HEK293/ABCB1 cells. These results suggested that tepotinib can inhibit the efflux function of ABCB1 transporter, thus increase the accumulation of chemotherapeutic drugs. As presented in **Fig.15A and C**, the intracellular levels of mitoxantrone in NCI-H460 and HEK293/pcDNA3.1 cells remained relatively constant throughout the 2 h incubation, both from 100% to 80%, and none of the inhibitors altered [^{3}H]-mitoxantrone accumulation level. In contrast, the intracellular level of mitoxantrone dropped significantly in NCI-H460/TPT10 and HEK293/ABCG2-WT cells (from 100% to 25% and from 100% to 40%, respectively), suggesting a large portion of mitoxantrone was pumped out by ABCG2. Importantly, the efflux of mitoxantrone was significantly inhibited with 3 μM of tepotinib or Ko143, while 1 μM of tepotinib inhibited the efflux process to a lesser extent. (**Fig.15B and D**).
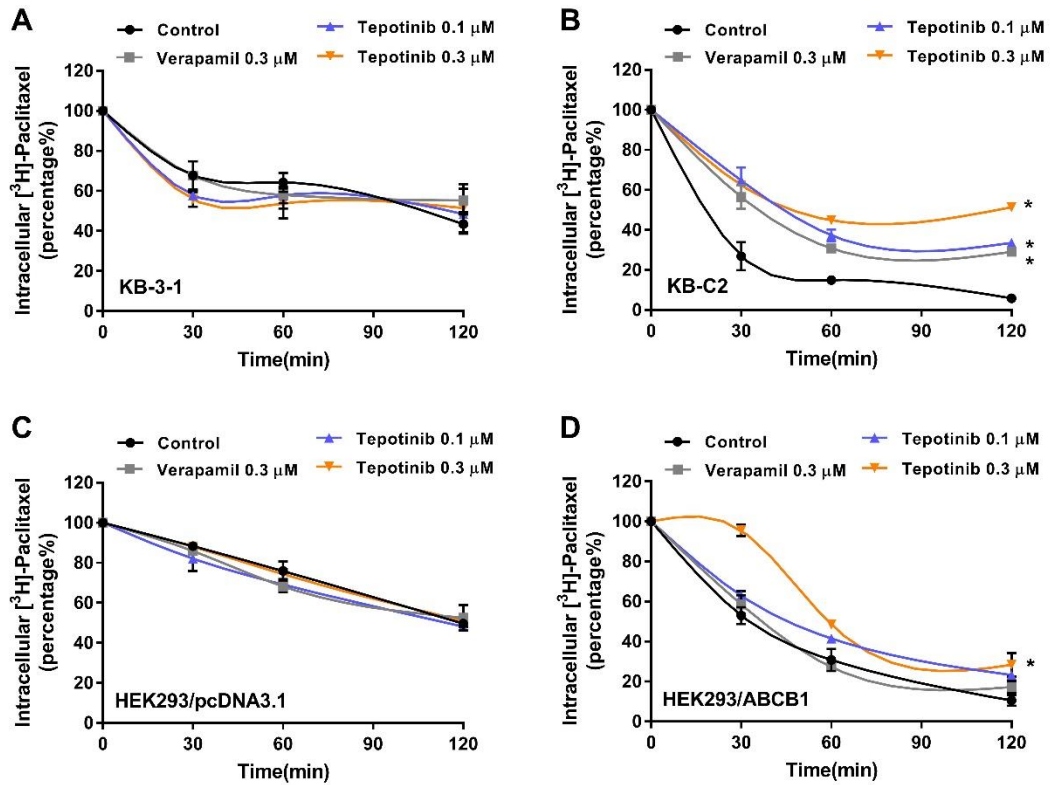
Figure 14. The effects of tepotinib on [³H]-paclitaxel efflux in ABCB1-overexpressing cells. (**A**) The efflux activities of [³H]-paclitaxel in (**A**) KB-3-1, (**B**) KB-C2, (**C**) HEK293/pcDNA3.1, and (**D**) HEK293/ABCB1 cells. Data are expressed as mean ± SD from three independent experiments (n=3). *p < 0.05 versus the corresponding control group.
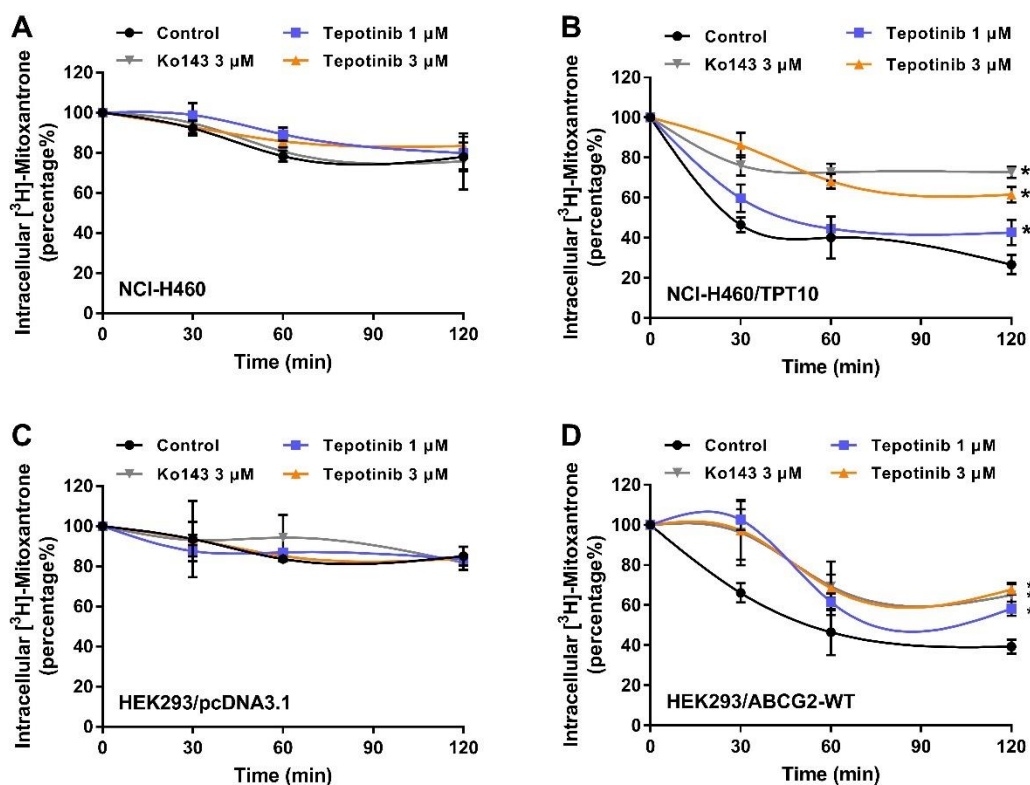
Figure 15. The effects of tepotinib on [3H]-mitoxantrone efflux in ABCG2-overexpressing cells. (**A**) The efflux activities of [3H]-mitoxantrone in (**A**) NCI-H460, (**B**) NCI-H460/TPT10, (**C**) HEK293/pcDNA3.1, and (**D**) HEK293/ABCG2-WT cells. Data are expressed as mean ± SD from three independent experiments (n=3). *$p < 0.05$ versus the corresponding control group.

3.11 Tepotinib Inhibited ABCB1/ABCG2 Efflux Activity in A Reversible Manner

In order to determine if tepotinib's inhibition of the efflux function of the ABCG2 and ABCB1 transporters is reversible or irreversible inhibition, we conducted an accumulation assay. Both KB-C2 and NCI-H460/TPT10 cancer cells were incubated in a pretreatment buffer with either tepotinib or positive inhibitor for 2 h. Subsequently, the cells were washed and incubated in an uptake buffer with [3H]-paclitaxel or [3H]-mitoxantrone with or without an inhibitor. The reversibility of the inhibitors was

assessed by comparing the intracellular accumulation level of [^{3}H]-paclitaxel and [^{3}H]-mitoxantrone. As shown in **Fig.16A**, the intracellular accumulation of [^{3}H]-paclitaxel was significantly increased in KB-C2 cells when 0.3 μM of tepotinib or verapamil were present in the pretreatment and uptake buffer, a finding that was consistent with our above-mentioned results. In contrast, the accumulation of [^{3}H]-paclitaxel was not significantly altered when only tepotinib or verapamil were present in the pretreatment buffer (**Fig.16A**). Verapamil is a reversible ABCB1 inhibitor and its MDR reversal efficacy is abrogated immediately after washout (84). These results suggest that tepotinib reversibly inhibits the efflux function of the ABCB1 transporter.

Similarly, the intracellular accumulation of [^{3}H]-mitoxantrone in NCI-H460/TPT10 cells was significantly increased when 3 μM of tepotinib or Ko143 were present in the pretreatment and uptake buffer (**Fig.16B**). When tepotinib or Ko143 were present in the pretreatment buffer only, the intracellular accumulation of [^{3}H]-mitoxantrone was not significantly altered. Ko143 is a reversible ABCG2 inhibitor and its inhibition efficacy decreases following repeated washings (85), indicating tepotinib also reversibly inhibits the efflux function of the ABCG2 transporter.
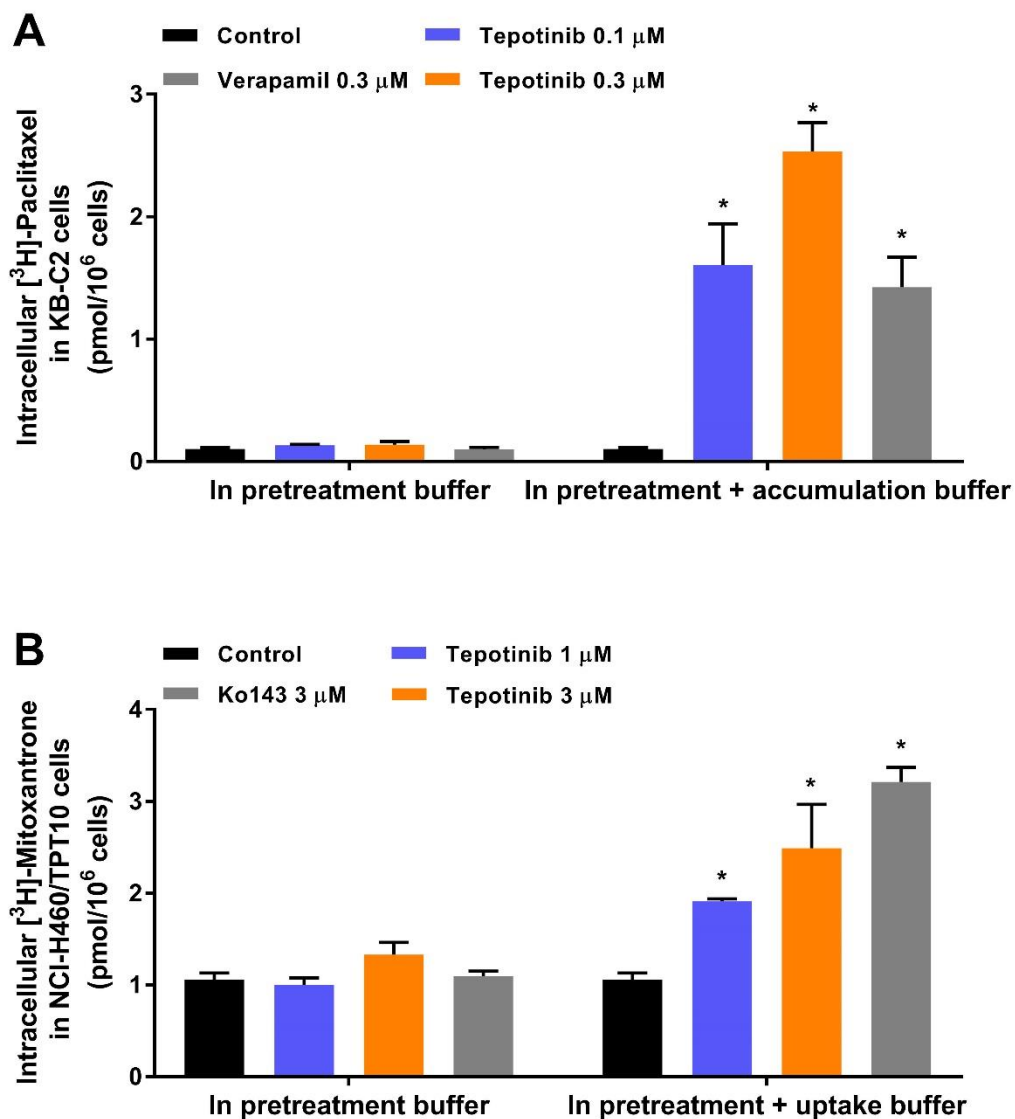
Figure 16. Tepotinib reversibly increased the accumulation of [^{3}H]-Substrate. (A) The intracellular accumulation of [^{3}H]-paclitaxel in KB-C2 cells after 2 h of pre-incubation with either vehicle, verapamil or tepotinib. (B) The intracellular accumulation of [^{3}H]-mitoxantrone in NCI-H460/TPT10 cells after 2 h of pre-incubation with either vehicle, Ko143 or tepotinib. Data are mean $\pm$ SD, representative of three independent experiments. *$p < 0.05$ versus the control group.

3.12 Docking Simulation of Tepotinib and ABCB1/ABCG2 Transporter

The binding modes of tepotinib with human homology ABCB1 and ABCG2 are depicted in **Fig.17**. Tepotinib shows good affinity with ABCB1 with a docking score of -14.343 kcal/mol. **Fig.17A** shows that one benzene ring of tepotinib has π-π interaction with the Phe302 residue of ABCB1. The remaining interaction of tepotinib and ABCB1 are hydrogen bonds formed by benzonitrile and Gln989, imide group and Asn720, pyrimidine ring and Gln837, piperidine ring and Asn295. Besides, tepotinib has hydrophobic interaction with the residues of ABCB1 including Ala291, Met298, Leu723, Phe769, Phe776, Ala833, Val 990 (**Fig. 17B**).

The interaction of tepotinib and ABCG2 are shown in **Fig.17D** (-11.620 kcal/mol). Compared with the interaction of tepotinib with ABCB1, tepotinib might has less interaction with ABCG2. The interaction between poziotinib and important residues of ABCG2 is presented in **Fig.17E**. The primary factors contributing to the binding of tepotinib to the ABCG2 transporter include π-π stacking by with Phe439 of ABCG2, and hydrophobic effect of the residues such as Ile543, Phe439, Val442, Met549, Phe432, Val546, Leu405 (**Fig.17E**).
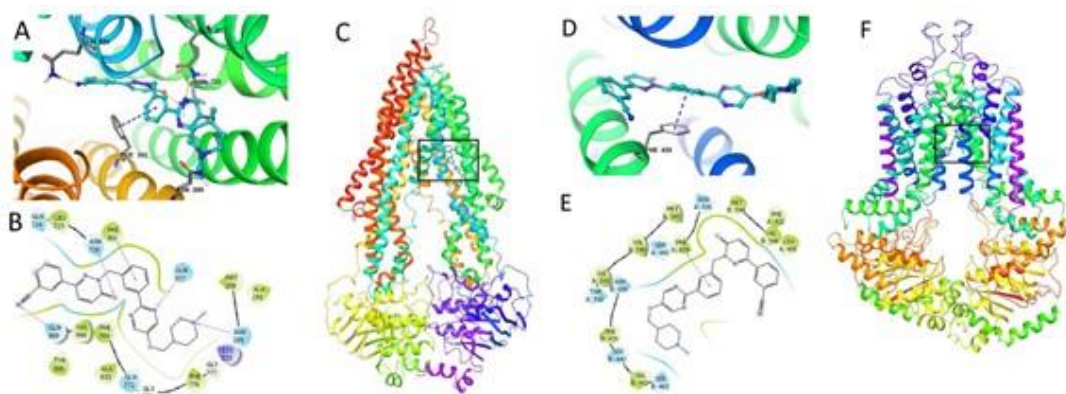
**Figure 17.** Molecular interaction of tepotinib with the human homology ABCB1 and ABCG2. (**A**) The three-dimensional ligand–receptor interaction diagram of tepotinib

and human ABCB1. Tepotinib is shown as ball and stick mode with the atoms colored: carbon – cyan, nitrogen – blue, oxygen – red. π-π stacking interactions are indicated with blue dotted line. Hydrogen bonds are indicated with yellow dotted line. (**B**) The two-dimensional ligand–receptor interaction graph of tepotinib and ABCB1. The amino acids within 3 Å are shown as colored bubbles: cyan – polar, green – hydrophobic. π-π stacking interactions are indicated with short green line. Hydrogen bonds are indicated with purple arrow. (**C**) The overall structure of human ABCB1 transporter. The square indicates the binding site of tepotinib. (**D**) The three-dimensional ligand–receptor interaction diagram of tepotinib and human ABCG2. (**E**) The two-dimensional ligand–receptor interaction graph of tepotinib and ABCG2. (**F**) The overall structure of human ABCG2. The square indicates the binding site.

3.13 The MDR Reversal Effect of Tepotinib in ABCG2 Tumor Xenograft Model

Based on the *in vitro* findings, we selected the tumor xenograft model to evaluate the ABCG2 reversal effect *in vivo*. In the parental NCI-H460 tumors (**Fig.18**), 30 mg/kg of tepotinib showed a moderate 27% inhibition ratio of tumor weight (IRW) and 14% inhibition ratio of tumor volume (IRV). In contrast, 3 mg/kg topotecan demonstrated 67% of IRW and IRV, while the combinational treatment did not enhance topotecan's antitumor effect. In the ABCG2-overexpressing NCI-H460/TPT10 tumors (**Fig.19**), tepotinib showed stronger antitumor effect compared to that in the parental tumors, with 49% IRW and 40% IRV. The antitumor effect of topotecan was attenuated, with 50% IRW and 40% IRV. The combinational treatment resulted in a more significant antitumor effect than the single treatments, showing 83% IRW and 88% IRV, which confirmed that tepotinib can antagonize ABCG2-mediated MDR and enhance the antitumor effect of topotecan.

Tepotinib was shown to be well-tolerated either as single treatment or as part of the combinational treatment since no obvious weight loss was observed (**Fig.20A**). The hematological parameters were evaluated in nude mice receiving different treatments (**Fig.20B**). The data show that both white blood cells and platelets counting were consistent between control and the treatment groups, suggesting tepotinib as an MDR reversal agent may not induce additional toxicity *in vivo*.
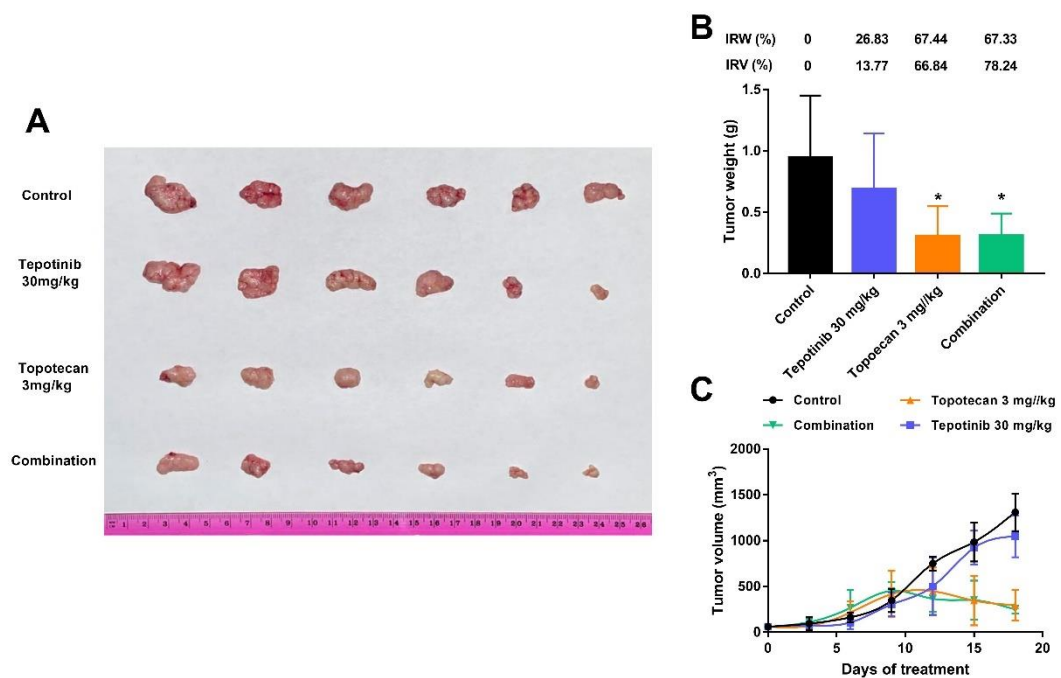
Figure 18. The effects of tepotinib on the antitumor effect of topotecan in NCI-H460 xenograft tumor models. (**A**) Images of excised NCI-H460 tumor tissues from nude athymic mice at the end of treatment period (n = 6). (**B**) The mean weight of excised NCI-H460 tumor tissues from the mice treated with vehicle, tepotinib, topotecan, or the combination. Ratio of growth inhibition (IR) for tumor weight (IRW) and tumor volume (IRV) are indicated. (**C**) The changes of tumor volume in NCI-H460 tumor xenograft model over time following the implantation. Data are expressed as mean ± SD from three independent experiments (n=3). *$p < 0.05$ versus the control group.
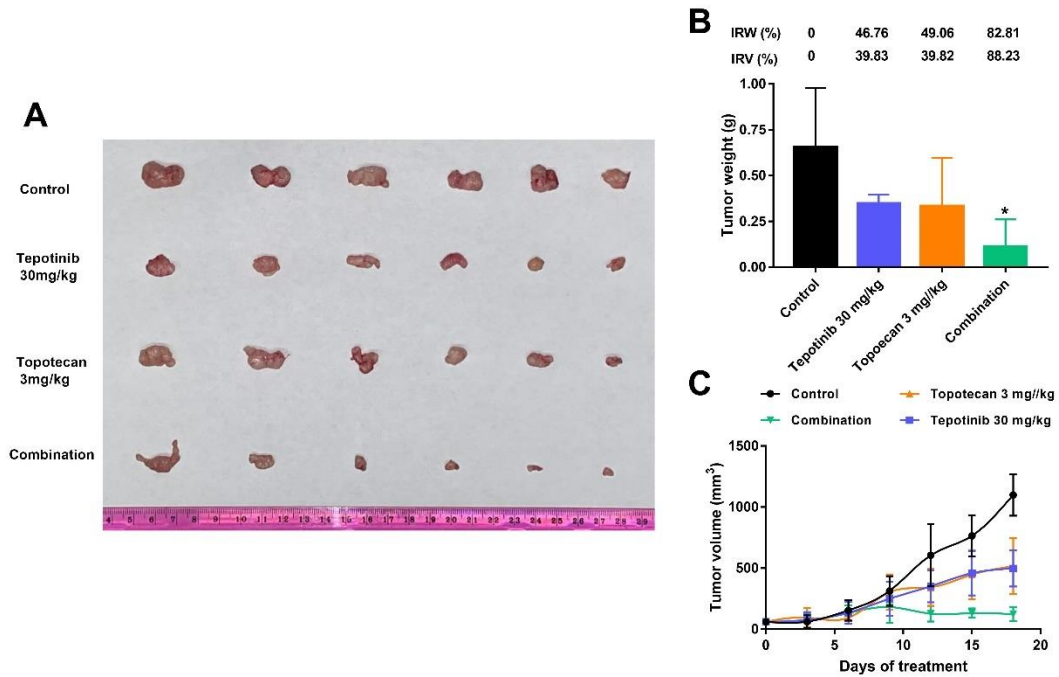
Figure 19. The effects of tepotinib on the antitumor effect of topotecan in NCI-H460/TPT10 xenograft tumor models. (**A**) Images of excised NCI-H460/TPT10 tumor tissues from nude athymic mice at the end of treatment period (n = 6). (**B**) The mean weight of excised NCI-H460/TPT10 tumor tissues from the mice treated with vehicle, tepotinib, topotecan, or the combination. Ratio of growth inhibition (IR) for tumor weight (IRW) and tumor volume (IRV) are indicated. (**C**) The changes of tumor volume in NCI-H460 tumor xenograft model over time following the implantation. Data are expressed as mean ± SD from three independent experiments (n=3). *p < 0.05 versus the control group.
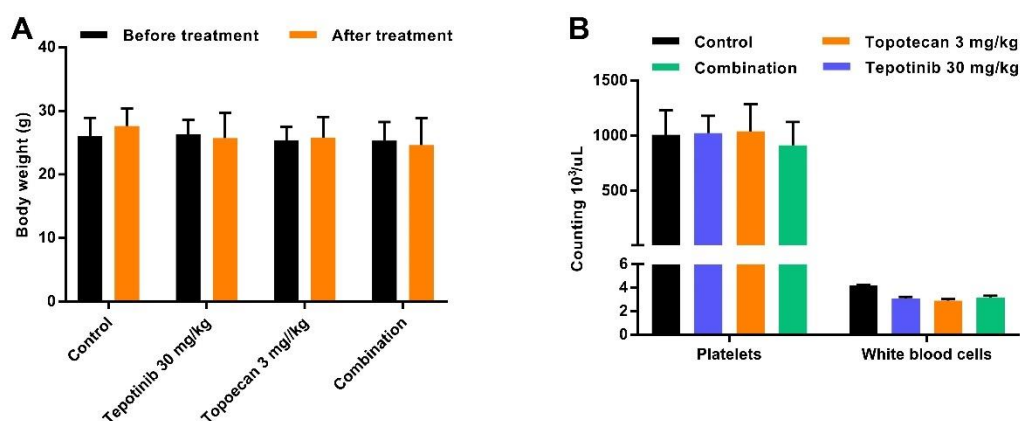
Figure 20. Tepotinib did not induce significant side effect in mice. (**A**) The changes of mean body weight before and after the study. (**B**) The counting of white blood cells and platelets in control and treatment groups. Data are expressed as mean ± SD from three independent experiments (n=3). *$p < 0.05$ versus the control group.

3.14 Plasma and Tumor Concentration of Tepotinib and Topotecan

To understand the pharmacokinetics of the drugs, HPLC analysis was applied to quantify the plasma and intratumoral concentrations of tepotinib and topotecan. The combinational treatment did not significantly alter the plasma concentrations of topotecan but increased the plasma concentrations of tepotinib (**Fig.21**). However, the tepotinib plasma concentration in combinational treatment decreased to the similar level of that in the single treatment at the end of 240 min evaluation. As shown in **Fig.22A**, the intratumoral level of tepotinib was increased in drug-resistant tumors compared to the parental tumors. The topotecan concentration in drug-resistant tumors decreased by 40% compared to the parental tumors, suggesting ABCG2 actively extruded topotecan from the tumors (**Fig.22B**). The combinational treatment did not significantly alter the topotecan level in parental tumors, but a 3-fold increase of topotecan concentration was observed in drug-resistant tumors.
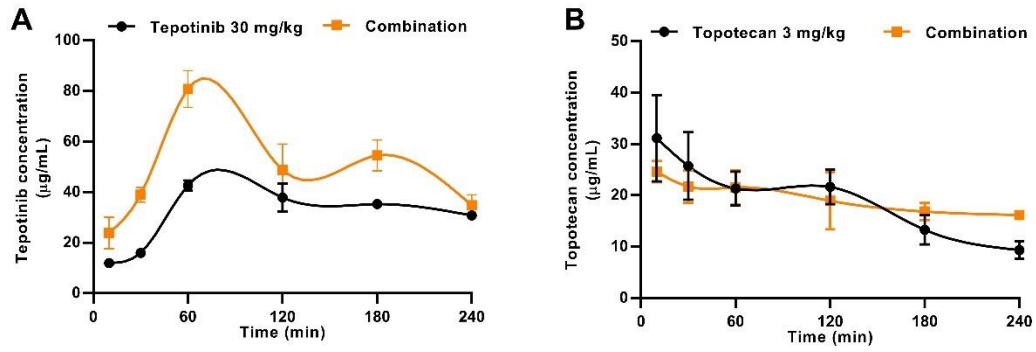
Figure 21. Plasma drug concentration in nude athymic mice in 240 min following administration of tepotinib alone or the combination. (**A**) Plasma concentration of tepotinib with single or combination treatment. (**B**) Plasma concentration of topotecan with single or combination treatment. Data are expressed as mean ± SD from three independent experiments (n=3). *p < 0.05 versus the control group.
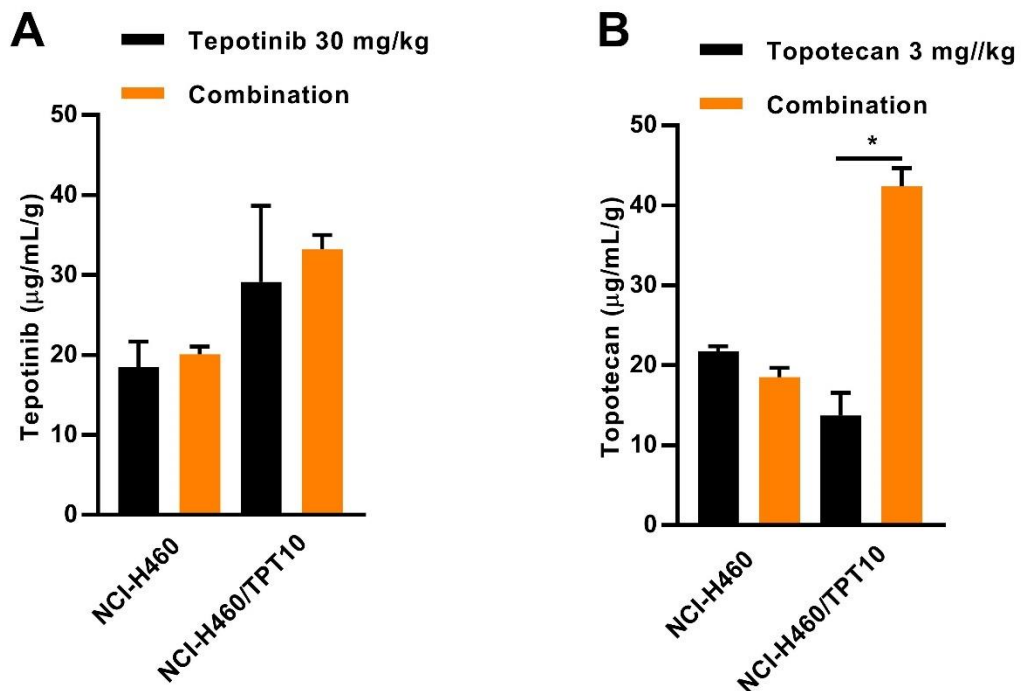
Figure 22. Intratumoral drug concentration in NCI-H460 and NCI-H460/TPT10 tumors. (**A**) Intratumoral concentration of tepotinib with single or combination

treatment. **(B)** Intratumoral concentration of topotecan with single or combination treatment. Data are expressed as mean ± SD from three independent experiments (n=3). *$p < 0.05$ versus the control group.

CHAPTER 4

**DISCUSSION**

Many studies have shown that the overexpression of ABCB1 and ABCG2 can induce MDR, which may lead to failure of chemotherapy (8). ABCB1 and ABCG2 transporters exert their protective function by pumping out xenobiotics but they may lead to MDR when overexpress in cancer cells. Because ABCB1/ABCG2 are important MDR mediator in cancer cells, tremendous effort has been made to develop effective reversal inhibitor to combat MDR. However, all clinical trials related to synthetic MDR inhibitors have failed due to the suboptimal efficacy and unacceptable adverse effects (86). Recent studies indicate that combining chemotherapeutic drugs with some TKIs could reverse ABCB1/ABCG2-mediated MDR (51). The rationale is to combine substrate drugs with an inhibitor, which inhibits the drug efflux process, thereby increasing the intracellular drug level and enhancing the anticancer efficacy (87). While the clinical investigation of reversal inhibitor did not meet the desired efficacy, it is still important to identify effective reversal inhibitors which allow future clinical investigations and predict potential drug-drug interactions.

Tepotinib is a MET TKI designated for NSCLC patients with METex14 mutations (88). It is currently approved for use in U.S and Japan for METex14-altered NSCLC patients. In addition, tepotinib is also under clinical investigation for hepatocellular carcinoma (NCT02115373, NCT01988493) and colorectal cancer (NCT04515394). Previous studies have shown that other MET TKIs, such as sitravatinib, alectinib, and glesatinib are able to antagonize ABCB1- and ABCG2-mediated MDR *in vitro* and *in vivo* (89). Therefore, it is tempting to evaluate if tepotinib has the similar MDR reversal effect. Here, we identified and characterized tepotinib as an effective reversal inhibitor against ABCB1- and ABCG2-mediated MDR.

To determine the nontoxic concentrations for MDR reversal studies, the

cytotoxicity profile was first evaluated in parental and drug-resistant cancer cells (**Fig.1B**). Based on the IC_{20} values, 3 μM of tepotinib was the highest nontoxic concentration to conduct the MDR reversal studies. A major finding of our study is that tepotinib can concentration-dependently and specifically sensitize ABCB1- or ABCG2-overexpressing cancer cells to the corresponding ABCB1 substrate drugs (paclitaxel and vincristine) or ABCG2 substrate drugs (mitoxantrone and topotecan), demonstrated by the decreased IC_{50} values of these substrate drugs in the drug-resistant cancer cells. Notably, tepotinib at 0.3 μM was sufficient to induce significant reversal effect in ABCB1-overexpressing cancer cells, while it required 3 μM to achieve complete reversal effect in ABCG2-overexpressing cancer cells. Besides, tepotinib did not enhance the anticancer efficacy of cisplatin, a non-substrate drug, in parental and drug-resistant cells. Moreover, the reversal effect was not observed in the parental or the gene-knockout cancer cells that have no ABCB1/ABCG2 protein expression, a result consistent with their non-drug resistant phenotype. Therefore, the results suggest that the reversal effect is specific to ABCB1 and ABCG2 transporters.

Our findings were further confirmed in gene-transfected HEK293 cells. Unlike drug-selected cancer cells, which could become drug resistant due to numerous mechanisms or pathways, the gene-transfected cells should only be resistant to ABCG2 and ABCB1 substrates by overexpressing the ABCG2 or ABCB1 transporters. Our results suggest that tepotinib can effectively reverse ABCB1-mediated MDR in HEK293/ABCB1 cells and the reversal efficacy is much higher than the positive inhibitor verapamil. For ABCG2 transporter, it has been shown that mutations at residue 482 can produce conformational changes that affect the binding of drugs and the efflux capacity of the ABCG2 transporter (90). For example, the two ABCG2 variants R482G and R482T were unable to transport methotrexate, while ABCG2-WT showed no

50

resistance to the lipophilic antifolate (91, 92). In addition, mitoxantrone is found to be a substrate of all ABCG2 variates, but rhodamine 123, daunorubicin are transported by only ABCG2 variants R482G or R482T. Tepotinib produced a concentration-dependent increase in the efficacy of mitoxantrone and topotecan in the HEK293 cells transfected with *ABCG2* gene containing the R482G and R482T mutations. Although the majority of ABCG2 inhibitors have reversal efficacy regardless of the mutation at residue 482, certain TKIs may have selective reversal effect for the ABCG2-WT or mutant variants. For instance, venetoclax (93), AC220 (94) and novobiocin (95) have been reported to reverse ABCG2-WT-mediated MDR but have no significant effect on the MDR mediated by the ABCG2 mutant variants. This is in contrast to tepotinib, which completely reversed MDR in HEK293 cells transfected with the ABCG2-WT or ABCG2 mutant variants. In the ABCB1/ABCG2 double-transfected HEK293 cells, tepotinib was able to significantly decrease the resistance fold of doxorubicin (from 45-fold to 3.6-fold), which is stronger than verapamil, a known ABCB1 inhibitor (from 45-fold to 6.6-fold) or ABCG2 inhibitor Ko143 (from 45-fold to 9.4-fold), suggesting that tepotinib may serve as a dual ABCB1/ABCG2 inhibitor. Previous studies found that the primitive leukemic CD34+/38- cells express high levels of ABCB1, ABCC1, and ABCG2 (96). The co-expression of MDR-related ABC transporters in cancer cells may require simultaneous modulation of multiple ABC transporters to achieve optimal inhibition and a better clinical outcome (97, 98). Our results confirmed that tepotinib can effectively antagonize ABCB1- and ABCG2-mediated MDR within clinically reachable concentrations, proposing tepotinib as a candidate inhibitor of ABCB1 and ABCG2. The combination of tepotinib with chemotherapeutic drugs or TKIs that are substrates of ABCB1/ABCG2 may benefit a subset of cancer patients with MDR tumor expressing both ABCB1 and ABCG2 transporters.

Taken together, we hypothesized that tepotinib can effective reverse MDR by interacting with ABCB1 and ABCG2 transporters. Subsequently, we conducted experiments to delineate or ascertain the MDR reversal mechanisms of tepotinib. Several potential mechanisms are proposed for reversal inhibitor, including 1) downregulating the protein expression of the transporter, 2) translocating the transporter from cell membrane to cytoplasm, and 3) directly inhibiting transporter from extruding the substrates. To this end, Western blot and immunofluorescence assay were carried out to evaluate if tepotinib affects to the protein expression or localization. The assays were carried out by incubating drug-resistant cancer cells with the highest reversal concentration of tepotinib for 72 h, which is the same strategy used in the cytotoxicity assay. The results show that tepotinib did not affect the protein expression level or membrane localization of ABCB1 and ABCG2 transporter. Instead, cellular thermal shift assay results suggest that tepotinib treatment can stabilize ABCB1 and ABCG2 protein against high temperatures compared to the solvent control DMSO. The ligand-bound protein generally has a higher thermal stability compared to unbound form, thus tepotinib may directly bind to the drug-binding site of ABCB1 and ABCG2 transporters.

Subsequently, we conducted an ATPase assay to further validate whether tepotinib has direct interaction with ABCB1/ABCG2 transporter. It is widely known that ABC transporters eliminate xenobiotics using the energy derived from ATP hydrolyzation. Certain reversal inhibitors are shown to either inhibit or stimulate the ABCB1/ABCG2 ATPase. Inhibiting the ATPase activity will attenuate the substrate efflux function since ABC transporter requires ATP hydrolysis to facilitate the drug translocation, such as tariquidar and dacomitinib (99, 100). If an inhibitor stimulates the ATPase activity, it is possible that the inhibitor can bind to the drug-binding site of the transporter, preventing

the binding and efflux of other substrate drugs. According to the results, tepotinib inhibited the ABCB1 ATPase activity in a concentration-dependent manner, which means that tepotinib may suppress the ATP hydrolysis process. Paclitaxel is a known substrate of ABCB1 that can stimulate the ATPase activity. When combined with paclitaxel, tepotinib was able to suppress the stimulated ATPase activity, suggesting tepotinib as an ABCB1 ATPase inhibitor. In contrast, tepotinib stimulated ABCG2 ATPase in a concentration-dependently manner, suggesting that tepotinib may bind to the drug-binding site and hinder the substrate efflux function of the transporter.

After confirming the interactions of tepotinib with ABCB1 and ABCG2 transporters, $[^3H]$-substrate accumulation and efflux assays were performed to characterize the interactions in-depth. The results show that tepotinib can increase the intracellular accumulation of $[^3H]$-paclitaxel and $[^3H]$-mitoxantrone in drug-resistant KB-C2 and NCI-H460/TPT10 cancer cells, respectively. However, this effect was not observed in the parental KB-3-1 and NCI-H460 cancer cells, since these two cell lines do not overexpress any ABC transporters. The effect was validated in HEK293 cells transfected with empty vector pcDNA3.1, *ABCB1* or *ABCG2* gene, suggesting that tepotinib increase $[^3H]$-substrate accumulation by interacting with ABCB1/ABCG2 transporters. To determine whether the tepotinib-ABCB1/ABCG2 interactions are reversible or irreversible, another $[^3H]$-substrate accumulation assay was performed using ABCB1-overexpressing KB-C2 and ABCG2-overexpressing NCI-H460/TPT10 cells. During the pretreatment incubation, tepotinib is purposed to bind to the transporter. When drug-resistant cells are incubated with tepotinib and $[^3H]$-substrate, the intracellular $[^3H]$-substrate accumulation increased significantly due to the inhibition of transporter. In contrast, when tepotinib was removed from the medium, the effect was abolished and the intracellular $[^3H]$-substrate level was identical to the

control group. Therefore, the results indicate that tepotinib binds to ABCB1/ABCG2 transporters in a reversible manner and the continuously presence of tepotinib is necessary to exert the MDR reversal effect.

Given that tepotinib may have increased the accumulation of [^{3}H]-substrates by increasing their entry and/or decreasing their efflux, we determined the effect of tepotinib on the efflux of [^{3}H]-substrates in the drug resistant cancer cells and gene-transfected cells. A shown in **Fig.19 and 20**, the vehicle-treated drug-resistant cells demonstrated active drug efflux process as indicated by the gradual decreasing of intracellular [^{3}H]-substrate accumulation. Since the [^{3}H]-substrate was removed from the medium, the reduction of [^{3}H]-substrate concentration is due solely to the efflux activity of ABCB1/ABCG2 transporters. Tepotinib was able to inhibit the [^{3}H]-substrate efflux process in drug-resistant cancer cells and gene-transfected cells without affecting that in the parental cells which does not overexpress any ABC transporter.

Taken together, the *in vitro* data confirm that tepotinib can effectively reversal both ABCB1- and ABCG2-mediated MDR in cancer cells. For ABCB1 transporter, tepotinib is able to inhibit the ABCB1 ATPase function, which limits the energy for ABCB1 efflux activity and thus increase the cellular retention of substrate drugs. For ABCG2 transporter, tepotinib can directly bind to the substrate-binding site of the transporter, which stimulate the ABCG2 ATPase activity. A recent study revealed that ABCG2 inhibitors such as Ko143 and tariquidar would tightly bind to the transmembrane domain of ABCG2, thereby blocking access for substrates (101). Thus, tepotinib hinder the substrate binding cycle of ABCG2 transporter, thereby facilitating the accumulation of substrate drugs, and enhancing their cytotoxicity in drug-resistant cells.

The *in-silico* docking simulation is an approach that has been widely used to predict the interaction of ligands with proteins (102). Although this technique may not

be indicative of the actual binding of a ligand to a protein, it can be used to identify compounds that interact with the substrate-drug binding site in ABC transporters (103, 104). Our docking analysis indicated that tepotinib interacted with the homology models of the ABCB1 (-6.6 kcal/mol) and ABCG2 (-10.1 kcal/mol) transporters. The lower docking score of poziotinib for the ABCG2 transporter compared to the ABCB1 transporter could be due to it forming a greater number of hydrophobic bonds with the ABCG2 transporter. In the ABCB1 docking analysis, the score of tepotinib was higher than other ABCB1 reversal agents such as CGM-097 (-8.5 kcal/mol), erdafitinib (-8.5 kcal/mol) and verapamil (-7.376 kcal/mol) (105, 106). Since the ABCB1 protein model was in complex with the ABCB1 inhibitor zosuquidar, there is an indication that tepotinib may have similar interaction with ABCB1 as other third-generation ABCB1 inhibitors. The docking score of tepotinib was comparable with other ABCG2 inhibitors, such as venetoclax (−12.1 kcal/mol) and sitravatinib (-13.248 kcal/mol) (93, 104). Furthermore, the docking results suggested that tepotinib interacts with the substrate-drug binding sites in the ABCB1 and ABCG2 proteins, a finding that supports our *in vitro* data indicating that tepotinib inhibits the efflux activity of these transporters.

Based on the *in vitro* findings, we selected the tumor xenograft model to translate the MDR reversal effect *in vivo*. Since the ABCG2 inhibitors are less developed compared to ABCB1 inhibitors, we primarily investigated the ABCG2 reversal effect of tepotinib in xenograft model. The oral administration of 30 mg/kg of tepotinib remarkably enhanced the antitumor efficacy of ABCG2 substrate drug topotecan (3 mg/kg i.p.). Since toxicity is a major issue for chemotherapeutic drug, the body weight of mice was close monitored during the process of this experiment. No noticeable change of body weight, WBC and platelets was recorded between the treatment groups and the control group. The reading of WBC and platelets had no significant alteration

after single or combination treatments, and the values are in accordance with the merchant's phenotypic data. The pharmacokinetic data show that the combination treatment did not affect the plasma or intratumoral level of topotecan in the parental NCI-H460 tumors. In contrast, the intratumoral topotecan concentration was upregulated in the drug-resistant NCI-H460/TPT10 tumors when receiving combination treatment. Therefore, the results suggest that tepotinib can effectively inhibit the ABCG2 efflux function and reverse MDR *in vivo*. Interestingly, the intratumoral level of tepotinib was higher in the drug-resistant tumors than the parental tumors, which may account for the enhanced antitumor effect in drug-resistant tumors. However, the underlying mechanism is inconclusive and desire further investigation.

CHAPTER 5

CONCLUSION

ABCB1/ABCG2-associated MDR remains one of the major issues of cancer treatment despite the development of new anticancer drugs. In this study, we repurpose the MET kinase inhibitor tepotinib as a dual inhibitor of ABCB1/ABCG2. The combination of tepotinib with ABCB1 substrate drugs paclitaxel and vincristine or ABCG2 substrate drugs mitoxantrone and topotecan shows improved anticancer effect in drug-resistant cancer cells. Importantly, overexpression of ABCB1, ABCG2, or ABCC1 transporters does not confer cancer cells drug resistance to tepotinib. Mechanistically, tepotinib hinders the substrate efflux activity of ABCB1 by inhibiting the ABCB1 ATPase function, thereby increasing the intracellular substrate concentration and enhancing the cytotoxic effect of substrate drugs in drug-resistant cancer cells. Besides, tepotinib reverses ABCG2-mediated MDR by directly binding to the substrate-binding site of ABCG2 transporter, thus interfering with the substrate binding process and increasing the substrate accumulation in cancer cells. Using gene-transfected and gene-knockout cell lines, we confirmed that the MDR reversal effect of tepotinib can be mainly attribute to specific inhibition of ABCB1 and ABCG2 transporters. Both Western blot and immunofluorescence assays suggest that tepotinib does not alter the protein expression or membrane localization of ABCB1/ABCG2 transporters. Moreover, tepotinib, at 30 mg/kg, has significant MDR reversal effect in ABCG2-overexpressing tumors *in vivo*. Taken together, this study provides a new potential strategy and the rationale of combining tepotinib with substrate drugs to combat ABCB1- or ABCG2-mediated MDR.

REFERENCES

1. Siegel RL, Miller KD, Fuchs HE, Jemal A. Cancer statistics, 2022. 2022;72(1):7-33.
2. Wu ZX, Yang Y, Wang JQ, Zhou WM, Chen J, Fu YG, et al. Elevated ABCB1 Expression Confers Acquired Resistance to Aurora Kinase Inhibitor GSK-1070916 in Cancer Cells. Frontiers in pharmacology. 2020;11:615824.
3. Wu Q, Yang Z, Nie Y, Shi Y, Fan D. Multi-drug resistance in cancer chemotherapeutics: mechanisms and lab approaches. Cancer Lett. 2014;347(2):159-66.
4. Krishna R, Mayer LD. Multidrug resistance (MDR) in cancer. Mechanisms, reversal using modulators of MDR and the role of MDR modulators in influencing the pharmacokinetics of anticancer drugs. European journal of pharmaceutical sciences : official journal of the European Federation for Pharmaceutical Sciences. 2000;11(4):265-83.
5. Elie Dassa PB. The ABC of ABCs: a phylogenetic and functional classification of ABC systems in living organisms. Research in microbiology. 2001;152:211-29.
6. Zhang YK, Wang YJ, Gupta P, Chen ZS. Multidrug Resistance Proteins (MRPs) and Cancer Therapy. AAPS J. 2015;17(4):802-12.
7. Beretta GL, Cassinelli G, Pennati M, Zuco V, Gatti L. Overcoming ABC transporter-mediated multidrug resistance: The dual role of tyrosine kinase inhibitors as multitargeting agents. Eur J Med Chem. 2017;142:271-89.
8. Stavrovskaya AA, Stromskaya TP. Transport proteins of the ABC family and multidrug resistance of tumor cells. Biochemistry (Moscow). 2008;73(5):592-604.
9. Daood M, Tsai C, Ahdab-Barmada M, Watchko JF. ABC transporter (P-gp/ABCB1, MRP1/ABCC1, BCRP/ABCG2) expression in the developing human CNS. Neuropediatrics. 2008;39(4):211-8.
10. Robert W. Robey KMP, Matthew D. Hall, Antonio T. Fojo, Susan E. Bates, Michael M. Gottesman,. Revisiting the role of ABC transporters in multidrug-resistant cancer. Nature Reviews Cancer. 2018;18(7):452-64.
11. Lin EW, Karakasheva TA, Hicks PD, Bass AJ, Rustgi AK. The tumor microenvironment in esophageal cancer. Oncogene. 2016;35(41):5337-49 %U http://www.nature.com/articles/onc201634.
12. Wang J, Yang DH, Yang Y, Wang JQ, Cai CY, Lei ZN, et al. Overexpression of ABCB1 Transporter Confers Resistance to mTOR Inhibitor WYE-354 in Cancer Cells. International journal of molecular sciences. 2020;21(4).
13. Wu ZX, Yang Y, Teng QX, Wang JQ, Lei ZN, Wang JQ, et al. Tivantinib, A c-Met Inhibitor in Clinical Trials, Is Susceptible to ABCG2-Mediated Drug Resistance. Cancers. 2020;12(1).
14. Robey RW, Pluchino KM, Hall MD, Fojo AT, Bates SE, Gottesman MM. Revisiting the role of ABC transporters in multidrug-resistant cancer. Nat Rev Cancer. 2018;18(7):452-64.
15. Fan Y, Mansoor N, Ahmad T, Wu ZX, Khan RA, Czejka M, et al. Enzyme and Transporter Kinetics for CPT-11 (Irinotecan) and SN-38: An Insight on Tumor Tissue Compartment Pharmacokinetics Using PBPK. Recent patents on anti-cancer drug discovery. 2019;14(2):177-86.
16. Chen XY, Yang Y, Wang JQ, Wu ZX, Li J, Chen ZS. Overexpression of ABCC1 Confers Drug Resistance to Betulin. Frontiers in oncology. 2021;11:640656.
17. Wu ZX, Teng QX, Cai CY, Wang JQ, Lei ZN, Yang Y, et al. Tepotinib reverses ABCB1-mediated multidrug resistance in cancer cells. Biochemical pharmacology. 2019;166:120-7.

18. Nosol K, Romane K, Irobalieva RN, Alam A, Kowal J, Fujita N, et al. Cryo-EM structures reveal distinct mechanisms of inhibition of the human multidrug transporter ABCB1. Proceedings of the National Academy of Sciences of the United States of America. 2020;117(42):26245-53.

19. Linton KJ, Higgins CF. Structure and function of ABC transporters: the ATP switch provides flexible control. Pflugers Arch. 2007;453(5):555-67.

20. Linton KJ. Structure and Function of ABC Transporters. Physiology. 2007;22(2):122-30.

21. Wu CP, S VA. The pharmacological impact of ATP-binding cassette drug transporters on vemurafenib-based therapy. Acta Pharm Sin B. 2014;4(2):105-11.

22. Sauna ZE, Smith MM, Müller M, Kerr KM, Ambudkar SVJJob, biomembranes. The mechanism of action of multidrug-resistance-linked P-glycoprotein. 2001;33 6:481-91.

23. Liu Y-S, Hsu H-C, Tseng K-C, Chen H-C, Chen S-J. Lgr5 promotes cancer stemness and confers chemoresistance through ABCB1 in colorectal cancer. Biomedicine & Pharmacotherapy. 2013;67(8):791-9.

24. Choudhuri S, Klaassen CD. Structure, function, expression, genomic organization, and single nucleotide polymorphisms of human ABCB1 (MDR1), ABCC (MRP), and ABCG2 (BCRP) efflux transporters. International journal of toxicology. 2006;25(4):231-59.

25. de Gooijer MC, Zhang P, Thota N, Mayayo-Peralta I, Buil LC, Beijnen JH, et al. P-glycoprotein and breast cancer resistance protein restrict the brain penetration of the CDK4/6 inhibitor palbociclib. Investigational new drugs. 2015;33(5):1012-9.

26. Rajamani BM, Benjamin ESB, Abraham A, Ganesan S, Lakshmi KM, Anandan S, et al. Plasma imatinib levels and ABCB1 polymorphism influences early molecular response and failure-free survival in newly diagnosed chronic phase CML patients. Scientific reports. 2020;10(1):20640.

27. Doyle LA, Yang W, Abruzzo LV, Krogmann T, Gao Y, Rishi AK, et al. A multidrug resistance transporter from human MCF-7 breast cancer cells. Proceedings of the National Academy of Sciences of the United States of America. 1998;95(26):15665-70.

28. Miyake K, Mickley L, Litman T, Zhan Z, Robey R, Cristensen B, et al. Molecular Cloning of cDNAs Which Are Highly Overexpressed in Mitoxantrone-resistant Cells. Demonstration of Homology to ABC Transport Genes. 1999;59(1):8-13.

29. Jackson SM, Manolaridis I, Kowal J, Zechner M, Taylor NMI, Bause M, et al. Structural basis of small-molecule inhibition of human multidrug transporter ABCG2. Nature structural & molecular biology. 2018;25(4):333-40.

30. Fletcher JI, Williams RT, Henderson MJ, Norris MD, Haber M. ABC transporters as mediators of drug resistance and contributors to cancer cell biology. Drug resistance updates : reviews and commentaries in antimicrobial and anticancer chemotherapy. 2016;26:1-9.

31. Ho MM, Ng AV, Lam S, Hung JY. Side population in human lung cancer cell lines and tumors is enriched with stem-like cancer cells. Cancer Res. 2007;67(10):4827-33.

32. Mao Q, Unadkat JD. Role of the breast cancer resistance protein (BCRP/ABCG2) in drug transport--an update. The AAPS journal. 2015;17(1):65-82.

33. Wei LY, Wu ZX, Yang Y, Zhao M, Ma XY, Li JS, et al. Overexpression of ABCG2 confers resistance to pevonedistat, an NAE inhibitor. Experimental cell research. 2020;388(2):111858.

34. Estevinho MM, Fernandes C, Silva CJ, Gomes CA, Afecto E, Correia J, et al. Role of ATP-binding Cassette Transporters in Sorafenib Therapy for Hepatocellular Carcinoma: An Overview. Current drug targets. 2021;22:1-12.

35. Fujita K-i, Hirose T, Kusumoto S, Sugiyama T, Shirai T, Nakashima M, et al. High exposure to erlotinib and severe drug-induced interstitial lung disease in patients with non-small-cell lung cancer. Lung Cancer. 2014;86(1):113-4.

36. Cole SP, Bhardwaj G, Gerlach JH, Mackie JE, Grant CE, Almquist KC, et al. Overexpression of a transporter gene in a multidrug-resistant human lung cancer cell line. Science (New York, NY). 1992;258(5088):1650-4.

37. Wang L, Johnson ZL, Wasserman MR, Levring J, Chen J, Liu S. Characterization of the kinetic cycle of an ABC transporter by single-molecule and cryo-EM analyses. eLife. 2020;9.

38. Borst P, Evers R, Kool M, Wijnholds J. A Family of Drug Transporters: the Multidrug Resistance-Associated Proteins. JNCI: Journal of the National Cancer Institute. 2000;92(16):1295-302.

39. Bakos E, Evers R, Szakács G, Tusnády GE, Welker E, Szabó K, et al. Functional multidrug resistance protein (MRP1) lacking the N-terminal transmembrane domain. The Journal of biological chemistry. 1998;273(48):32167-75.

40. Eckford PD, Sharom FJ. ABC efflux pump-based resistance to chemotherapy drugs. Chemical reviews. 2009;109(7):2989-3011.

41. Deeley RG, Cole SP. Substrate recognition and transport by multidrug resistance protein 1 (ABCC1). FEBS letters. 2006;580(4):1103-11.

42. Ishikawa T. The ATP-dependent glutathione S-conjugate export pump. Trends in biochemical sciences. 1992;17(11):463-8.

43. Wilson CS, Davidson GS, Martin SB, Andries E, Potter J, Harvey R, et al. Gene expression profiling of adult acute myeloid leukemia identifies novel biologic clusters for risk classification and outcome prediction. Blood. 2006;108(2):685-96.

44. Liu B, Li LJ, Gong X, Zhang W, Zhang H, Zhao L. Co-expression of ATP binding cassette transporters is associated with poor prognosis in acute myeloid leukemia. Oncology letters. 2018;15(5):6671-7.

45. Patel C, Stenke L, Varma S, Lindberg ML, Björkholm M, Sjöberg J, et al. Multidrug resistance in relapsed acute myeloid leukemia: evidence of biological heterogeneity. Cancer. 2013;119(16):3076-83.

46. Bartholomae S, Gruhn B, Debatin KM, Zimmermann M, Creutzig U, Reinhardt D, et al. Coexpression of Multiple ABC-Transporters is Strongly Associated with Treatment Response in Childhood Acute Myeloid Leukemia. Pediatric blood & cancer. 2016;63(2):242-7.

47. Ji N, Yang Y, Cai CY, Lei ZN, Wang JQ, Gupta P, et al. VS-4718 Antagonizes Multidrug Resistance in ABCB1- and ABCG2-Overexpressing Cancer Cells by Inhibiting the Efflux Function of ABC Transporters. Front Pharmacol. 2018;9:1236.

48. Wu S, Fu L. Tyrosine kinase inhibitors enhanced the efficacy of conventional chemotherapeutic agent in multidrug resistant cancer cells. Mol Cancer. 2018;17(1):25.

49. Wang YJ, Zhang YK, Zhang GN, Al Rihani SB, Wei MN, Gupta P, et al. Regorafenib overcomes chemotherapeutic multidrug resistance mediated by ABCB1 transporter in colorectal cancer: In vitro and in vivo study. Cancer Lett. 2017;396:145-54.

50. Zhang XY, Zhang YK, Wang YJ, Gupta P, Zeng L, Xu M, et al. Osimertinib (AZD9291), a Mutant-Selective EGFR Inhibitor, Reverses ABCB1-Mediated Drug Resistance in Cancer Cells. Molecules. 2016;21(9).

51. Zhang YK, Zhang GN, Wang YJ, Patel BA, Talele TT, Yang DH, et al. Bafetinib (INNO-406) reverses multidrug resistance by inhibiting the efflux function of ABCB1 and ABCG2 transporters. Sci Rep. 2016;6:25694.

52. Eadie LN, Hughes TP, White DL. Interaction of the efflux transporters ABCB1 and

ABCG2 with imatinib, nilotinib, and dasatinib. Clin Pharmacol Ther. 2014;95(3):294-306.

53. Bladt F, Faden B, Friese-Hamim M, Knuehl C, Wilm C, Fittschen C, et al. EMD 1214063 and EMD 1204831 constitute a new class of potent and highly selective c-Met inhibitors. Clin Cancer Res. 2013;19(11):2941-51.

54. Li J, Kwok HF. Current Strategies for Treating NSCLC: From Biological Mechanisms to Clinical Treatment. Cancers. 2020;12(6).

55. Ma PC, Jagadeeswaran R, Jagadeesh S, Tretiakova MS, Nallasura V, Fox EA, et al. Functional Expression and Mutations of c-Met and Its Therapeutic Inhibition with SU11274 and Small Interfering RNA in Non–Small Cell Lung Cancer. 2005;65(4):1479-88.

56. Xu X, Yao L. Recent Patents on the Development of c-Met Kinase Inhibitors. Recent patents on anti-cancer drug discovery. 2020.

57. Organ SL, Tsao M-S. An overview of the c-MET signaling pathway. 2011;3(1_suppl):S7-S19.

58. Salgia R. MET in Lung Cancer: Biomarker Selection Based on Scientific Rationale. 2017;16(4):555-65.

59. Fujino T, Suda K, Mitsudomi T. Emerging MET tyrosine kinase inhibitors for the treatment of non-small cell lung cancer. Expert opinion on emerging drugs. 2020:1-21.

60. Onozato R, Kosaka T, Kuwano H, Sekido Y, Yatabe Y, Mitsudomi T. Activation of MET by Gene Amplification or by Splice Mutations Deleting the Juxtamembrane Domain in Primary Resected Lung Cancers. Journal of Thoracic Oncology. 2009;4(1):5-11.

61. Abella JV, Peschard P, Naujokas MA, Lin T, Saucier C, Urbé S, et al. Met/Hepatocyte growth factor receptor ubiquitination suppresses transformation and is required for Hrs phosphorylation. Molecular and cellular biology. 2005;25(21):9632-45.

62. Huang C, Zou Q, Liu H, Qiu B, Li Q, Lin Y, et al. Management of Non-small Cell Lung Cancer Patients with MET Exon 14 Skipping Mutations. Current treatment options in oncology. 2020;21(4):33.

63. Bladt F, Faden B, Friese-Hamim M, Knuehl C, Wilm C, Fittschen C, et al. EMD 1214063 and EMD 1204831 Constitute a New Class of Potent and Highly Selective c-Met Inhibitors. 2013;19(11):2941-51.

64. Underiner TL, Herbertz T, Miknyoczki SJ. Discovery of small molecule c-Met inhibitors: Evolution and profiles of clinical candidates. Anti-cancer agents in medicinal chemistry. 2010;10(1):7-27.

65. Mikami K, Medová M, Nisa L, Francica P, Glück AA, Tschan MP, et al. Impact of p53 Status on Radiosensitization of Tumor Cells by MET Inhibition-Associated Checkpoint Abrogation. Molecular cancer research : MCR. 2015;13(12):1544-53.

66. Nisa L, Francica P, Giger R, Medo M, Elicin O, Friese-Hamim M, et al. Targeting the MET Receptor Tyrosine Kinase as a Strategy for Radiosensitization in Locoregionally Advanced Head and Neck Squamous Cell Carcinoma. Molecular cancer therapeutics. 2020;19(2):614-26.

67. Falchook GS, Hong DS, Amin HM, Fu S, Piha-Paul SA, Janku F, et al. Results of the first-in-human phase I trial assessing MSC2156119J (EMD 1214063), an oral selective c-Met inhibitor, in patients (pts) with advanced solid tumors. Journal of Clinical Oncology. 2014;32(15_suppl):2521-.

68. Bladt F, Blaukat A, Dorsch D, Fittschen C, Friese-Hamim M, Graedler U, et al. Abstract 3622: Preclinical characterization of EMD1214063, a potent and highly selective inhibitor of the c-Met kinase in Phase I clinical trials. Cancer Research.

2010;70(8 Supplement):3622.

69. Falchook GS, Kurzrock R, Amin HM, Fu S, Piha-Paul SA, Janku F, et al. Efficacy, safety, biomarkers, and phase II dose modeling in a phase I trial of the oral selective c-Met inhibitor tepotinib (MSC2156119J). Journal of Clinical Oncology. 2015;33(15_suppl):2591-.

70. Paik PK, Felip E, Veillon R, Sakai H, Cortot AB, Garassino MC, et al. Tepotinib in Non-Small-Cell Lung Cancer with MET Exon 14 Skipping Mutations. The New England journal of medicine. 2020;383(10):931-43.

71. Zaal EA, Berkers CR. The Influence of Metabolism on Drug Response in Cancer. 2018;8(500).

72. Hu G, Han C, Wild CP, Hall J, Chen J. Lack of effects of selenium on <i>N</i> -nitrosomethylbenzylamine-induced tumorigenesis, DNA methylation, and oncogene expression in rats and mice. Nutrition and Cancer. 1992;18(3):287-95 %U http://www.tandfonline.com/doi/abs/10.1080/01635589209514229.

73. Lai GM, Chen YN, Mickley LA, Fojo AT, Bates SE. P-glycoprotein expression and schedule dependence of adriamycin cytotoxicity in human colon carcinoma cell lines. International journal of cancer. 1991;49(5):696-703.

74. Lei ZN, Teng QX, Wu ZX, Ping FF, Song P, Wurpel JND, et al. Overcoming multidrug resistance by knockout of ABCB1 gene using CRISPR/Cas9 system in SW620/Ad300 colorectal cancer cells. MedComm. 2021;2(4):765-77.

75. Raymond M. Lyall JH, Carol Cardarelli, David FitzGerald, Shin-Ichi Akiyama, Michael M. Gottesman, Ira Pastan. Isolation of Human KB Cell Lines Resistant to Epidermal Growth Factor-Pseudomonas Exotoxin Conjugates. Cancer research. 1987;47:2961-6.

76. Taguchi Y, Yoshida A, Takada Y, Komano T, Ueda K. Anti-cancer drugs and glutathione stimulate vanadate-induced trapping of nucleotide in multidrug resistance-associated protein (MRP). FEBS Letters. 1997;401(1):11-4.

77. Ciruelos E, Villagrasa P, Pascual T, Oliveira M, Pernas S, Paré L, et al. Palbociclib and Trastuzumab in HER2-Positive Advanced Breast Cancer: Results from the Phase II SOLTI-1303 PATRICIA Trial. 2020;26(22):5820-9.

78. Wu Z-X, Teng Q-X, Yang Y, Acharekar N, Wang J-Q, He M, et al. MET inhibitor tepotinib antagonizes multidrug resistance mediated by ABCG2 transporter: In vitro and in vivo study. Acta Pharmaceutica Sinica B. 2021.

79. Robinson AN, Tebase BG, Francone SC, Huff LM, Kozlowski H, Cossari D, et al. Coexpression of ABCB1 and ABCG2 in a Cell Line Model Reveals Both Independent and Additive Transporter Function. Drug metabolism and disposition: the biological fate of chemicals. 2019;47(7):715-23.

80. Narayanan S, Gujarati NA, Wang J-Q, Wu Z-X, Koya J, Cui Q, et al. The Novel Benzamide Derivative, VKNG-2, Restores the Efficacy of Chemotherapeutic Drugs in Colon Cancer Cell Lines by Inhibiting the ABCG2 Transporter. 2021;22(5):2463.

81. Wang JQ, Wang B, Lei ZN, Teng QX, Li JY, Zhang W, et al. Derivative of 5-cyano-6-phenylpyrimidin antagonizes ABCB1- and ABCG2-mediated multidrug resistance. European journal of pharmacology. 2019;863:172611.

82. Ji N, Yang Y, Cai C-Y, Lei Z-N, Wang J-Q, Gupta P, et al. Selonsertib (GS-4997), an ASK1 inhibitor, antagonizes multidrug resistance in ABCB1- and ABCG2-overexpressing cancer cells. Cancer Letters. 2019;440-441:82-93.

83. Alam A, Küng R, Kowal J, McLeod RA, Tremp N, Broude EV, et al. Structure of a zosuquidar and UIC2-bound human-mouse chimeric ABCB1. Proceedings of the National Academy of Sciences. 2018;115:E1973-E82.

84. Newman MJ, Rodarte JC, Benbatoul KD, Romano SJ, Zhang C, Krane S, et al.

Discovery and characterization of OC144-093, a novel inhibitor of P-glycoprotein-mediated multidrug resistance. Cancer research. 2000;60(11):2964-72.

85. Ozvegy-Laczka C, Várady G, Köblös G, Ujhelly O, Cervenak J, Schuetz JD, et al. Function-dependent conformational changes of the ABCG2 multidrug transporter modify its interaction with a monoclonal antibody on the cell surface. The Journal of biological chemistry. 2005;280(6):4219-27.

86. Robey RW, Pluchino KM, Hall MD, Fojo AT, Bates SE, Gottesman MM. Revisiting the role of ABC transporters in multidrug-resistant cancer. Nature Reviews Cancer. 2018;18(7):452-64.

87. Zhang L, Li Y, Wang Q, Chen Z, Li X, Wu Z, et al. The PI3K subunits, P110α and P110β are potential targets for overcoming P-gp and BCRP-mediated MDR in cancer. Molecular Cancer. 2020;19(1):10.

88. Wu ZX, Li J, Dong S, Lin L, Zou C, Chen ZS. Tepotinib hydrochloride for the treatment of non-small cell lung cancer. Drugs of today (Barcelona, Spain : 1998). 2021;57(4):265-75.

89. Yang Y, Ji N, Teng Q-X, Cai C-Y, Wang J-Q, Wu Z-X, et al. Sitravatinib, a Tyrosine Kinase Inhibitor, Inhibits the Transport Function of ABCG2 and Restores Sensitivity to Chemotherapy-Resistant Cancer Cells in vitro. 2020;10.

90. Ejendal KF, Diop NK, Schweiger LC, Hrycyna CA. The nature of amino acid 482 of human ABCG2 affects substrate transport and ATP hydrolysis but not substrate binding. Protein science : a publication of the Protein Society. 2006;15(7):1597-607.

91. Chen ZS, Robey RW, Belinsky MG, Shchaveleva I, Ren XQ, Sugimoto Y, et al. Transport of methotrexate, methotrexate polyglutamates, and 17beta-estradiol 17-(beta-D-glucuronide) by ABCG2: effects of acquired mutations at R482 on methotrexate transport. Cancer research. 2003;63(14):4048-54.

92. Bram E, Ifergan I, Shafran A, Berman B, Jansen G, Assaraf YG. Mutant Gly482 and Thr482 ABCG2 mediate high-level resistance to lipophilic antifolates. Cancer chemotherapy and pharmacology. 2006;58(6):826-34.

93. Wang JQ, Li JY, Teng QX, Lei ZN, Ji N, Cui Q, et al. Venetoclax, a BCL-2 Inhibitor, Enhances the Efficacy of Chemotherapeutic Agents in Wild-Type ABCG2-Overexpression-Mediated MDR Cancer Cells. Cancers. 2020;12(2).

94. Li J, Kumar P, Anreddy N, Zhang YK, Wang YJ, Chen Y, et al. Quizartinib (AC220) reverses ABCG2-mediated multidrug resistance: In vitro and in vivo studies. Oncotarget. 2017;8(55):93785-99.

95. Robey RW, Honjo Y, Morisaki K, Nadjem TA, Runge S, Risbood M, et al. Mutations at amino-acid 482 in the ABCG2 gene affect substrate and antagonist specificity. British journal of cancer. 2003;89(10):1971-8.

96. Raaijmakers MH, de Grouw EP, Heuver LH, van der Reijden BA, Jansen JH, Scheper RJ, et al. Breast cancer resistance protein in drug resistance of primitive CD34+38- cells in acute myeloid leukemia. Clinical cancer research : an official journal of the American Association for Cancer Research. 2005;11(6):2436-44.

97. Robey RW, Massey PR, Amiri-Kordestani L, Bates SE. ABC transporters: unvalidated therapeutic targets in cancer and the CNS. Anti-cancer agents in medicinal chemistry. 2010;10(8):625-33.

98. Raaijmakers MHGP. ATP-binding-cassette transporters in hematopoietic stem cells and their utility as therapeutical targets in acute and chronic myeloid leukemia. Leukemia. 2007;21(10):2094-102.

99. Fan YF, Zhang W, Zeng L, Lei ZN, Cai CY, Gupta P, et al. Dacomitinib antagonizes multidrug resistance (MDR) in cancer cells by inhibiting the efflux activity of ABCB1 and ABCG2 transporters. Cancer Lett. 2018;421:186-98.

100.   Chufan EE, Kapoor K, Ambudkar SV. Drug-protein hydrogen bonds govern the inhibition of the ATP hydrolysis of the multidrug transporter P-glycoprotein. Biochem Pharmacol. 2016;101:40-53.

101.   Jackson SM, Manolaridis I, Kowal J, Zechner M, Taylor NMI, Bause M, et al. Structural basis of small-molecule inhibition of human multidrug transporter ABCG2. Nature structural & molecular biology. 2018;25(4):333-40.

102.   Kontoyianni M. Docking and Virtual Screening in Drug Discovery. Methods in molecular biology (Clifton, NJ). 2017;1647:255-66.

103.   Ferreira RJ, Bonito CA, Cordeiro M, Ferreira MU, Dos Santos D. Structure-function relationships in ABCG2: insights from molecular dynamics simulations and molecular docking studies. Scientific reports. 2017;7(1):15534.

104.   Yang Y, Ji N, Teng QX, Cai CY, Wang JQ, Wu ZX, et al. Sitravatinib, a Tyrosine Kinase Inhibitor, Inhibits the Transport Function of ABCG2 and Restores Sensitivity to Chemotherapy-Resistant Cancer Cells in vitro. Frontiers in oncology. 2020;10:700.

105.   Feng W, Zhang M, Wu ZX, Wang JQ, Dong XD, Yang Y, et al. Erdafitinib Antagonizes ABCB1-Mediated Multidrug Resistance in Cancer Cells. Frontiers in oncology. 2020;10:955.

106.   Yang Y, Ji N, Cai C-Y, Wang J-Q, Lei Z-N, Teng Q-X, et al. Modulating the function of ABCB1: in vitro and in vivo characterization of sitravatinib, a tyrosine kinase inhibitor. Cancer Communications. 2020;40(7):285-300.

VITA

Name: Zhuoxun Wu

Baccalaureate Degree: Bachelor of Science, Guangdong

                                   Pharmaceutical University,

                                   Guangzhou, China, Major:

                                   Pharmacy

Date Graduated: June, 2017